






Laccaria bicolor pectin methylesterases are involved in ectomycorrhiza development with *Populus tremula* × *Populus tremuloides*

Jamil Chowdhury^{1,2} , Minna Kemppainen³ , Nicolas Delhomme¹ , Iryna Shutava², Jingjing Zhou^{1,2}, Junko Takahashi¹ , Alejandro G. Pardo³ and Judith Lundberg-Felten¹ 

¹Department of Forest Genetics and Plant Physiology, Umeå Plant Science Center, Swedish University of Agricultural Sciences, 90183 Umeå, Sweden; ²Department of Plant Physiology, Umeå Plant Science Center, Umeå University, 90187 Umeå, Sweden; ³Laboratory of Molecular Mycology, Department of Science and Technology, Institute of Basic and Applied Microbiology, National University of Quilmes (UNQ), and National Scientific and Technical Research Council (CONICET), B1876BXD Bernal, Argentina

Summary

Author for correspondence:
Judith Lundberg-Felten
Email: judith.lundberg-felten@slu.se

Received: 8 June 2022
Accepted: 29 June 2022

New Phytologist (2022) 236: 639–655
doi: 10.1111/nph.18358

Key words: cell wall, cell-wall remodelling, cell-wall-modifying enzymes, ectomycorrhiza, *Laccaria bicolor*, pectin, pectin methylesterase, *Populus*.

- The development of ectomycorrhizal (ECM) symbioses between soil fungi and tree roots requires modification of root cell walls. The pectin-mediated adhesion between adjacent root cells loosens to accommodate fungal hyphae in the Hartig net, facilitating nutrient exchange between partners. We investigated the role of fungal pectin modifying enzymes in *Laccaria bicolor* for ECM formation with *Populus tremula* × *Populus tremuloides*.
- We combine transcriptomics of cell-wall-related enzymes in both partners during ECM formation, immunolocalisation of pectin (Homogalacturonan, HG) epitopes in different methylesterification states, pectin methylesterase (PME) activity assays and functional analyses of transgenic *L. bicolor* to uncover pectin modification mechanisms and the requirement of fungal pectin methylesterases (LbPMEs) for ECM formation.
- Immunolocalisation identified remodelling of pectin towards de-esterified HG during ECM formation, which was accompanied by increased *LbPME1* expression and PME activity. Overexpression or RNAi of the ECM-induced *LbPME1* in transgenic *L. bicolor* lines led to reduced ECM formation. Hartig Nets formed with *LbPME1* RNAi lines were shallower, whereas those formed with *LbPME1* overexpressors were deeper.
- This suggests that *LbPME1* plays a role in ECM formation potentially through HG de-esterification, which initiates loosening of adjacent root cells to facilitate Hartig net formation.

Introduction

Ectomycorrhizal (ECM) symbiosis is one of the most predominant forms of plant–microbe interactions in boreal and temperate forest ecosystems (Read *et al.*, 2004; Qu *et al.*, 2010; McGuire *et al.*, 2013) in which it plays a key role in plant health through mineral nutrient cycling. During symbiosis establishment, ECM fungi form a sheath around the lateral root tips and colonise the apoplastic space between epidermal and cortical root cells (Kottke & Oberwinkler, 1987; Abras *et al.*, 1988), forming the Hartig net, a nutritional exchange site between plant and fungus. Formation of this symbiotic interface requires modification of plant and fungal cell walls (Brundrett, 2004; Martin *et al.*, 2017) and has interested researchers for > 30 yr (Paris *et al.*, 1993; Balestrini *et al.*, 1996; Balestrini & Bonfante, 2014). *In situ* immunolabelling-based characterisation of the cell-wall polymer epitopes (pectin, cellulose, hemicellulose) in mature ECM in comparison with nonmycorrhizal roots, has underpinned our understanding of how the plant cell wall is altered during the

establishment of hyphae in the apoplastic space. The suggested key mechanisms for Hartig net formation are (1) mechanical force from the hyphal tip (Garcia *et al.*, 2015), (2) auxin secretion from root tips to promote cell-wall loosening (Gea *et al.*, 1994) and (3) secretion of fungal cell-wall-degrading enzymes (CWDEs) (Bonfante & Genre, 2010; Veneault-Fourrey *et al.*, 2014). The two former hypotheses await further proof through functional studies, whereas the latter has largely benefitted from the availability of fungal genomes and the possibility of using RNAi techniques in the ectomycorrhizal model fungus *L. bicolor* to identify and functionally characterise potential fungal plant cell-wall degrading (PCWDE) enzymes (Zhang *et al.*, 2018, 2022). Whole-genome sequences of several ECM species have revealed that ECM fungi have a reduced set of PCWDEs compared with their saprotrophic ancestors (Martin *et al.*, 2008; Kohler *et al.*, 2015; Miyachi *et al.*, 2020). ECM fungi are likely to employ these PCWDEs to modify the plant cell-wall matrix for apoplastic accommodation to establish bi-directional nutrient transport. A significant increase of PCWDE expression during

ECM interactions further supports this hypothesis (Sebastiana *et al.*, 2014; Veneault-Fourrey *et al.*, 2014; Kohler *et al.*, 2015).

The extracellular route that fungal hyphae take during Hartig net formation is rich in pectic polysaccharides; in particular, homogalacturonan (HG) is predominant in the middle lamella between adjacent root cells (Daher & Braybrook, 2015). Pectic polysaccharides make up to 35% of the total cell-wall dry weight and play versatile roles in plant physiological processes including cell growth and differentiation. Their dynamic alterations can modify cell-wall chemistry and rheology (Bidhendi & Geitmann, 2016). HG modifying enzymes (HGMEs) play a central role in cell-to-cell adhesion and cell separation (Sénéchal *et al.*, 2014; Daher & Braybrook, 2015) and include multigenic families such as pectin methylsterases (PMEs), pectin acetylsterases (PAEs), pectate lyases (PLs) and polygalacturonases (PGs) (Sénéchal *et al.*, 2014). The ECM basidiomycete *Laccaria bicolor* has a restricted set of HGMEs comprising only four PMEs and six PGs (Martin *et al.*, 2008), of which the ECM-induced *LbGH28A* has recently been functionally characterised for its activity on pectin and polygalacturonic acid and is suggested to contribute to Hartig net formation (Zhang *et al.*, 2022). Conversely, its host plant *Populus tremula* has a large set of HGMEs comprising 73 PMEs, 12 PAEs, 28 PLs and 38 PGs (Sundell *et al.*, 2015). Despite the reduced HGME set, *L. bicolor* HGMEs, that is LbPMEs and LbPGs, are transcriptionally upregulated at various time points during an interaction with *Populus* (Veneault-Fourrey *et al.*, 2014; Kohler *et al.*, 2015; and the current study) suggesting their involvement in ECM development. PMEs seem to act as first modifiers of HG modification (Pelloux *et al.*, 2007; Manmohit Kalia, 2015; Sénéchal *et al.*, 2015) and catalyse the de-esterification of the C6-linked methyl-ester groups of HG chains. Although the exact modes of action of PMEs are still debated, PME-mediated HG de-esterification patterns can be random or blockwise, with enzyme isoforms and cell wall pH being determining factors (Catoire *et al.*, 1998; Denès *et al.*, 2000; Kim *et al.*, 2005). Therefore, depending on physiological conditions, PME activity regulates both cell-wall loosening and cell-wall stiffening (Micheli, 2001; Sénéchal *et al.*, 2014). During cell-wall loosening, PME de-esterification activity makes HG more accessible to depolymerising enzymes such as PLs and PGs (Micheli, 2001; Pelloux *et al.*, 2007; Sénéchal *et al.*, 2014; Manmohit Kalia, 2015). As it has recently been shown that a fungal PG (*LbGH28A*) is involved in Hartig net formation (Zhang *et al.*, 2022), we are here hypothesising that preceding steps of HG modification also receive a fungal contribution. Several fungal pathogens employ PMEs to overcome pectin-rich cell-wall barriers (Lionetti *et al.*, 2012; Sella *et al.*, 2016; Fan *et al.*, 2017). ECM fungi encoding PMEs may apply similar strategies to modify cell walls to form the Hartig net. We hypothesise that *L. bicolor* PMEs facilitate cell-wall loosening during ECM development. Therefore, we investigated the functional role of *L. bicolor* PMEs in ECM symbiosis. Using *L. bicolor* and *P. tremula* × *P. tremuloides* interactions in an *in vitro* culture system, we leveraged whole-genome transcriptomics, microscopy coupled with immunolabelling and transgenic approaches targeting LbPMEs to explore

the methylesterification state of plant cell walls in ECM and the potential role of *L. bicolor* PMEs during ECM formation.

Materials and Methods

Fungal strains and growth conditions

Laccaria bicolor (Maire) P.D. Orton, isolate S238N, empty vector lines EV7 and EV9 (Plett *et al.*, 2011) and transgenic lines (this study) were maintained on agar Pachlewski P5 medium at 20°C. For experiments, we used 14-d-old free-living mycelia (FLM) grown on cellophane placed on solidified Pachlewski P20 medium. For media and culture conditions please refer to Felten *et al.* (2009). *Populus tremula* L. × *Populus tremuloides* Michx. (T89) cuttings were micropropagated under *in vitro* conditions and grown on half strength Murashige and Skoog (½MS) medium (Murashige & Skoog, 1962) containing 2% sucrose and 1% plant agar (P1001; Duchefa Biochemie BV, Haarlem, the Netherlands) with pH 5.8 in rectangular 14 × 7.5 cm, 7.5 cm high pots under a 16 h photoperiod at 22°C. After 1 month, rooted cuttings were transferred to 12-cm square Petri dishes containing freshly prepared ½MS medium. The root systems were covered above and below with a cellophane membrane and grown vertically for 2 wk before we started interaction studies through an *in vitro* sandwich culture system on 2-ethanesulfonic acid (MES)-buffered P20 medium with cellophane-grown FLM, as described in Felten *et al.* (2009).

RNA extraction and cDNA synthesis

The time-course samples for RNA-sequencing data were derived from the *in vitro* sandwich culture of *L. bicolor* interacting with *P. tremula* × *P. tremuloides* as mentioned previously. Control plant and fungal samples were grown in separate plates without any interactions. At 3, 7, 14, 21 and 28 d after fungal contact (DAC) 10 root tips (ECM or control) each *c.* 0.5 cm long, were harvested from two plants per condition and pooled to be considered as one replicate. We analysed four such replicates per time point and condition. For FLM controls, young hyphae were collected at the periphery of fungal cultures without plants. Total RNA was extracted using the RNAqueous™ Total RNA Isolation Kit (Invitrogen) and following the manufacturer's instructions, except that 1% polyvinylpyrrolidone (PVP) was added to the extraction buffer. The remaining gDNA was removed using a DNA-free™ DNA Removal Kit (AM1906; ThermoScientific, Waltham, MA, USA) followed by purification of the RNA using an RNeasy MinElute Cleanup Kit (74204; Qiagen). RNA concentration and quality were checked using a NanoDrop 2000 spectrophotometer (Thermo Scientific) and using Bioanalyzer RNA 6000 pico chips (5067-1513; Agilent.com), respectively. Full-length cDNAs were generated according to the SMART-SEQ2 protocol (Picelli *et al.*, 2014) followed by quality control analysis using the Agilent High Sensitivity DNA Kit (5067-4626; Agilent.com). Sequencing libraries were generated using a Rubicon ThruPLEX DNA-seq kit (Takara Bio Inc., San Jose, CA, USA) and sequencing of all 55 samples took place on a single

Illumina NovaSeq6000 S2 flow-cell lane generating 150-bp paired-end reads at SciLifeLab (Science for Life Laboratory, Stockholm, Sweden).

For qPCR analysis, the procedures for RNA extraction from free-living mycelia, cDNA synthesis, conditions for qRT-PCR and gene-expression analysis are identical to those described in Kempainen *et al.* (2020). Four replicates per condition and genotype were assessed using qPCR analysis, except for the initial large-scale screening of transgenic fungal lines, in which only one biological replicate per line was analysed. The primer sequences used in the qRT-PCR expression analysis are provided in Supporting Information Table S1.

Preprocessing of RNA-seq data and differential expression analyses

Data preprocessing was performed as described by Delhomme *et al.* (2014). Details can be found in Methods S1. The raw data are available from the European Nucleotide Archive (ENA, <https://ebi.ac.uk/ena>) under the accession no. PRJEB41173.

PME activity assay

PME activity in the ECM and control plant root tips was measured in a coupled enzyme-based spectrophotometric assay (Grsic-Rausch & Rausch, 2004) on a spectrophotometric 96-well plate reader (Epoch; Biotek, Winooski, VT, USA). Starting material comprised 50 mg (FW) from each of five biological replicates of root/mycorrhizal samples. We measured PME activity in the FLM, following the method described by Anthon & Barrett (2004) with modifications to increase sensitivity and consistency (Methods S2).

Sample preparation for microscopy and immunolocalisation

The ECM and control root tips of *c.* 0.5 cm length were collected at 7, 14, 21 and 28 DAC. At each time point, we collected 10 to 12 root tips from five to six plants, fixed them in 4% paraformaldehyde in PBS overnight at 4°C, infiltrated and embedded them in LR white resin (hard grade) and used a glass knife microtome to make 1- μ m thick cross-sections following the protocol described by Burton *et al.* (2011). For immunolabelling, we localised pectin epitopes with antibodies (LM19 and LM20, that preferentially recognise de-esterified or highly methylesterified HG epitopes, respectively (Verhertbruggen *et al.*, 2009)) on three sequential cross-sections (considered as equivalent sections) cut at *c.* 500 μ m from the root apex following the protocol described by Chowdhury *et al.* (2014) except that we used the CyTM5-conjugated anti-rat secondary antibody and Alexa Fluor 488 conjugated with WGA for FLM labelling (Methods S3). For negative controls, sections were treated similarly except that the primary antibodies were not added. No fluorescence was visible (images were black) in negative controls. For ECM anatomy analysis, we used double staining with Alexa Fluor 488 conjugated with WGA (10 μ g ml⁻¹ final concentration) to reveal fungal tissues and, for the plant cell wall, 0.01% Pontamine fast

scarlet 4BS in PBS (Anderson *et al.*, 2010). For transmission electron microscopy, we localised pectin epitopes with LM19 and LM20 antibodies in 70-nm thick resin embedded sections, which were recognised by 5 nm gold conjugated anti-rat IgG secondary antibody (Wilson & Bacic, 2012) and visualised under a Talos L120C transmission electron microscope. Gold beads were quantified manually on 10–16 images from three individual root sections per antibody and condition.

Confocal image acquisition and image analysis

Images were acquired using a confocal laser scanning microscope (Zeiss LSM780) equipped with a \times 40 1.2 NA water immersion objective. The Alexa Fluor 488 conjugated with WGA and the CyTM5 conjugate with secondary antibody were excited with 488 nm and 633 nm laser lines and detected at 500–590 nm and 640–750 nm, respectively. We indirectly quantified pectin epitopes by measuring the fluorescence probe (Cy5) intensity (mean number of pixels per unit area) conjugated with the respective primary antibody using the ‘curve spline’ function of the ZEISS ZEN BLUE software. The intensity values were normalised by subtracting the background obtained from negative controls of equivalent sections.

PME vector construction and generation of *L. bicolor* PME transgenic lines

We created RNAi constructs driven by the constitutive *Agaricus bisporus gpdII* promoter and silencing either *LbPME1* (*LbPME1*_RNAi) or simultaneous silencing *LbPME1* and three highly similar *Laccaria* PMEs: *LbPME2* (JGIv2 ID #676331), *LbPME3* (JGIv2 ID #315258), *LbPME4* (JGIv2 ID #315313) (referred to as *LbPME1-4_double* RNAi) (Figs S1, S2). *L. bicolor* cloning and transformation (Kempainen *et al.*, 2005; Kempainen & Pardo, 2010), selection and insert number analysis using ddPCR (Glowacka *et al.*, 2016) and insertion site characterisation (Table S2) using plasmid rescue (Kempainen *et al.*, 2008) and TAIL PCR (Liu *et al.*, 1995, Liu & Chen, 2007) are described in detail in Methods S4–S7.

Results

Time-course gene-expression profiling reveals alteration of cell-wall modifying genes during *L. bicolor* and *P. tremula* \times *P. tremuloides* interactions

We performed a time-course gene-expression study using RNA-seq to reveal differentially expressed genes (DEGs) related to plant cell-wall modification in *P. tremula* \times *P. tremuloides* and *L. bicolor* at 3, 7, 14, 21 and 28 DAC in colonised lateral root tips or the respective controls (control root tips without fungus or free-living mycelium) (Tables S3–S6). These time points during ECM formation correspond to hyphal adhesion on the root (0–3 d), mantle formation (3–7 d), penetration of the root (7–14 d) and Hartig net maturation (21–28 d) (Fig. S3), as revealed using microscopic observation. *L. bicolor* and *P. tremula* \times *P.*

tremuloides cell-wall-related transcriptome profiles were markedly influenced by their interaction (Figs 1, S4–S6). A higher proportion of PCWDEs encoding genes related to pectin, hemicellulose and cellulose, were upregulated in the fungal genome (up to 68% upregulated genes in the respective family) compared with the plant genome (up to 12% upregulated genes in the respective families) (Figs S5, S6). None of the xylan modifying enzymes

present in *L. bicolor* or *Populus* was induced. Several homogalacturonan (HG) modifying enzymes were differentially expressed in both plant and fungus (Figs 2, S7). This included the specific upregulation of three out of 73 *Populus* PME1s at 3, 7 and 14 DAC and downregulation of seven *Populus* PME1s at 21 and 28 DAC. Only one of the four *L. bicolor* PME1s (*LbPME1*) showed significant upregulation at all time points (confirmed using

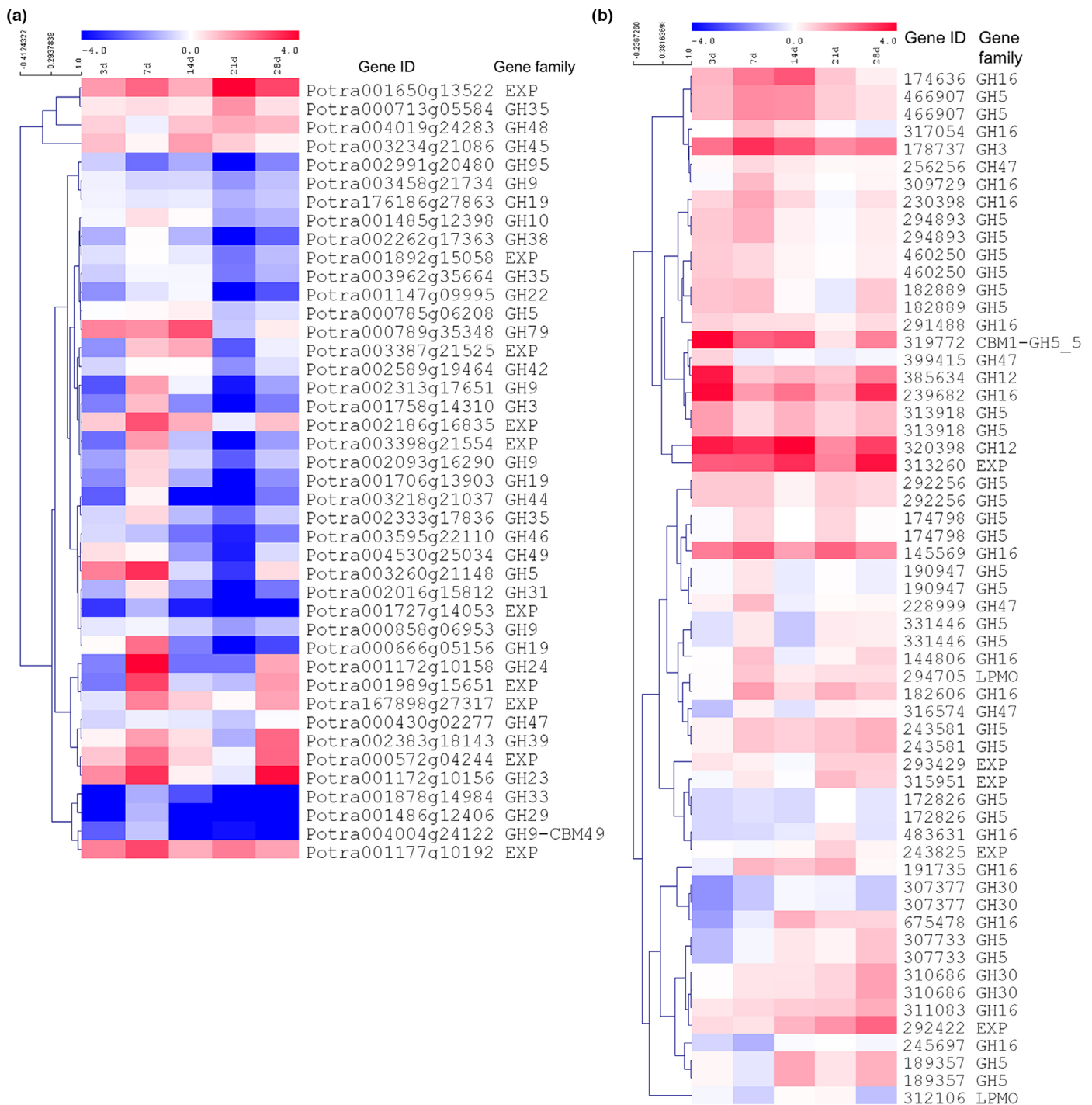
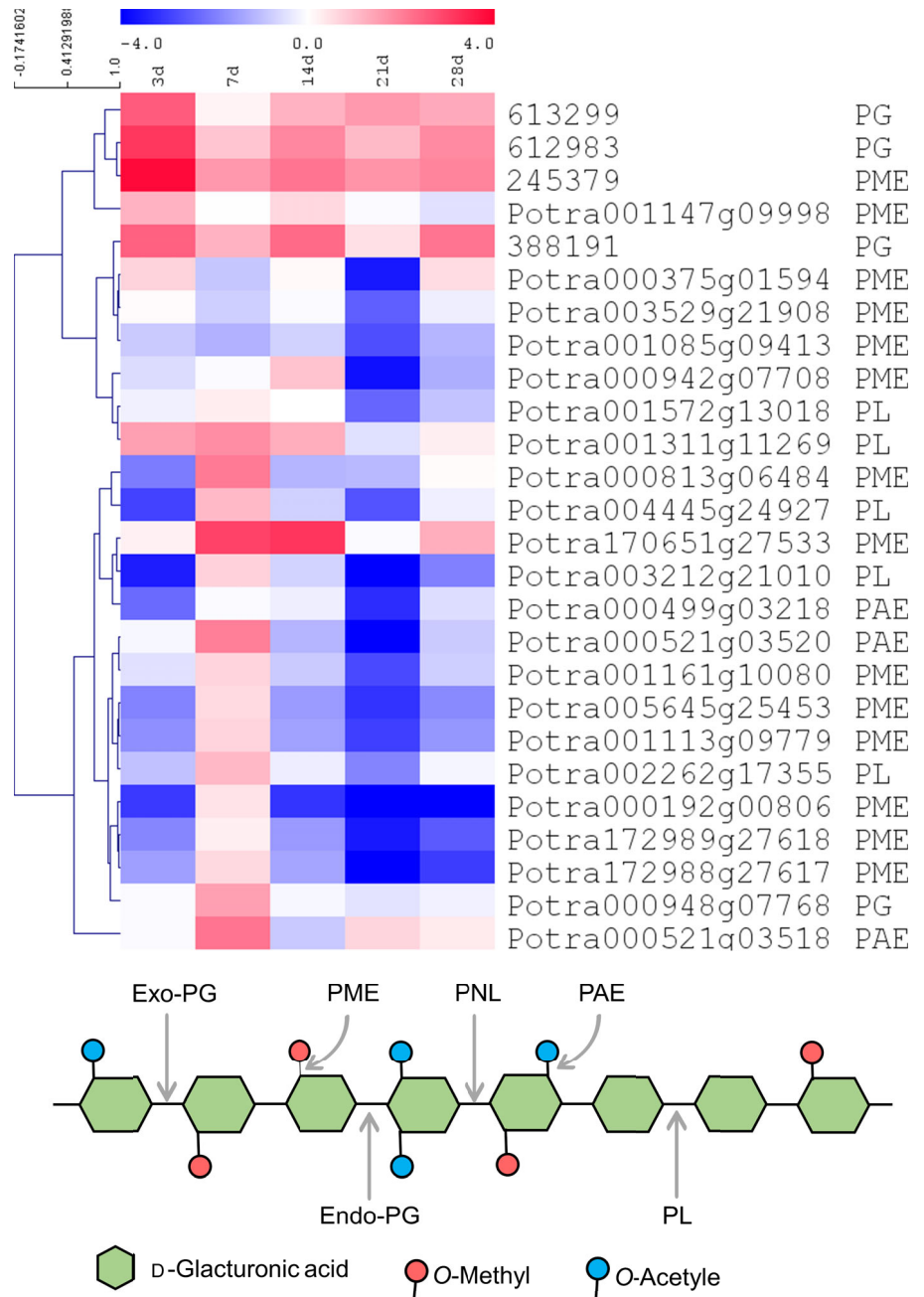


Fig. 1 Heat maps of relative gene-expression levels of differentially expressed genes (DEGs) related to cellulose and hemicellulose degrading enzymes in (a) *Populus tremula* × *Populus tremuloides* and (b) and *Laccaria bicolor*. Expression matrix of the log₂ fold change values cluster for gene based on Pearson's clustering method.

Fig. 2 Time-course RNA-seq expression profile of the potential candidate homogalacturonan (HG) modifying enzymes (HGMEs) during *Laccaria bicolor* interaction with *Populus tremula* × *Populus tremuloides*. The heat map represents log₂ fold change ratios of differentially regulated genes (log₂ fold change 0.5, *P*-adj < 0.05) in colonised roots vs control roots without fungus harvested at the respective similar time point. Fold change values are indicated. PME, pectin methylesterase; PMEI, pectin methylesterase inhibitor; PAE, pectin acetyltransferase; PG, polygalacturonase; PGI, polygalacturonase inhibitor; PL, pectate lyase; PNL, pectin lyase. Note that PMEI, PAE, PGI, PNL and PL gene families are absent in *L. bicolor*. Lower figure shows a representation of homogalacturonan and the cleavage sites of potential HGMEs.



qPCR; Fig. S8) whilst none of the others showed any changes (Figs 2, S7, S9). Our data also revealed differential expression of *Populus* PME inhibitors (PMEIs), an inhibitory protein family of plant PMEs (Di Matteo *et al.*, 2005; Wormit & Usadel, 2018), only during the late stages, at 21 DAC and 28 DAC, with two members being upregulated, and three members downregulated (Fig. S7). Plant PMEIs are unlikely to inhibit fungal PMEs due to the lack of conserved critical residues in fungal PMEs for a PME–PMEI interaction (Giovane *et al.*, 2004; Di Matteo *et al.*, 2005; Lionetti *et al.*, 2007; Reca *et al.*, 2012). Protein alignments confirmed the absence of the PME domain (PF04043) in *L. bicolor* PMEs (and a wide range of fungi with different lifestyles) (Fig. S10), suggesting that post-translational inhibition

of fungal PMEs by plant PMEIs is an unlikely event. The PME domain structure occurs as a contributing factor for phylogenetic clustering when plant and fungal PMEs are aligned (Fig. S10a).

De-esterification by PMEs precedes HG degradation by the activity of HG depolymerising enzymes such as polygalacturonases (PGs) or pectin lyases (PNLs) (Sénéchal *et al.*, 2014). Our transcriptome profiles showed a significant upregulation of only one out of 38 *Populus* PGs, but three out of six *L. bicolor* PGs during the interaction. Interestingly, we also noted the upregulation of three *Populus* PG inhibitors (PGIs), which could potentially influence both plant and fungal PG activity (Federici *et al.*, 2001; Protsenko *et al.*, 2008; Benedetti *et al.*, 2011). Although PNLs appear to be absent from the *Populus* genome,

one *Populus* PL was upregulated at 7 DAC and four *Populus* PLs were downregulated at 21 DAC, whereas PLs are not present in *L. bicolor*. Similarly, only one *Populus* pectin acetyltransferase (PAE) was upregulated at 7 DAC and four *Populus* PAEs were downregulated at 21 DAC; this group of enzymes was again not detected in *L. bicolor*. Altogether, our transcriptome analysis revealed ECM-specific regulation of HG modifying gene family members associated with HG de-esterification, deacetylation and depolymerisation during *L. bicolor* and *P. tremula* × *P. tremuloides* interactions. Concerning potential HG biosynthesis genes in *Populus*, only one galacturonosyltransferase was upregulated, the others were downregulated (Fig. S11). We did not find any differential expression of *Populus* pectin methyl transferases (Fig. S11). Therefore, the data are inconclusive regarding whether pectin synthesis in *Populus* is affected by ECM formation.

Comparing our data to two published datasets of time-course gene-expression profiles during *Populus*–*L. bicolor* interactions in a soil system (Veneault-Fourrey *et al.*, 2014; Plett *et al.*, 2015), we noticed an overlap of the differentially expressed LbCAZymes in both our and the previous studies (Fig. S12). Out of our 63 *L. bicolor* CAZYMes that were differentially expressed at least one time point in our study, 33 (Veneault-Fourrey & Martin, 2011; Veneault-Fourrey *et al.*, 2014) and 45 (Plett *et al.*, 2015) were respectively found to overlap with our results (Table S7). However, none of the differentially expressed *Populus* CAZYMes (Table S8) from our study was detected in the other studies, probably due to the use of a different *Populus* hybrid in our study. Interestingly, among the overlapping LbCAZYMes, a majority corresponded to genes induced during the late phases of ECM formation in soil systems (clusters C and D in Veneault-Fourrey *et al.* (2014)). This can be explained by the fact that, in soil systems, only few hyphae are in contact with the plant in the early stages, whereas these phases progress much more quickly in *in vitro* systems. The majority of genes (33 out of 45; Fig. S12) that overlapped with LbDEGs in Plett *et al.* (2015) belonged to what they identified as regulon L_H and were those significantly differentially regulated during the aggregation phase and maintained their regulation until time points for mature ECM in association with *P. trichocarpa* in this report.

Pectin de-esterification during ECM development

To decipher the spatial and temporal HG methylesterification patterns during ECM formation we used immunofluorescence microscopy with LM19 and LM20 antibodies that bind preferentially to de-esterified HG or highly methylesterified HG, respectively (Verherbruggen *et al.*, 2009). In radial walls between adjacent epidermal cells, which loosens during Hartig net formation, the abundance of LM19 epitopes was visually higher, and the one of LM20 epitopes was lower in sections through ECM roots (14 DAC) compared with similar tissues in control roots (Fig. 3a–d, arrowed). In control roots the LM19 signal was patchy and mostly visible at cell corners and in the tangential wall separating epidermis and cortex cells (Fig. 3a), whereas in ECM sections the signal was strong and

homogenous all around the epidermis cells (Fig. 3c). Labelling with LM20, conversely, gave a more homogenous signal in the epidermis of control root sections (Fig. 3b) and decreased in the epidermis and the outermost cortex layer of ECM sections to a signal almost solely visible in the cell corners (Fig. 3d). Quantification of the LM19:LM20 ratio confirmed that *in situ* methylesterification levels were significantly modified in ECM compared with control roots. There was a significant increase in the LM19:LM20 ratio from 7 DAC onwards both in the epidermal layer (Fig. 3e), which is in physical contact with the fungus, and even in underlying root cells (Fig. 3f). Similar observations were made in successive sections taken at 100- μ m intervals between 150 μ m and 550 μ m from the root tip (Fig. S13). This suggests that HG undergoes de-esterification throughout ECM development starting before Hartig net formation, as concluded from the 7 DAC time point when only a fungal mantle but no Hartig net is however present (Fig. S3). Transmission electron micrographs (TEM), coupled with immunogold labelling, confirmed that increased levels of LM19 epitopes were present in the plant cell wall within the Hartig net compared with the epidermal wall of the control roots (Fig. S14, quantified in Fig. S15). We observed that LM19 epitopes were mainly limited to the interface of plant and fungal cell walls and were absent from fungal cell walls and from the space between adjacent fungal cells in the Hartig net. The increased abundance of de-esterified HG was accompanied by a significantly increased PME activity in 14 DAC colonised roots (with contributions from both plant and fungal PMEs) compared with control roots or FLM in two separate experiments (Fig. S16).

Transgenic alteration of *L. bicolor* PME transcripts alters PME activity level

To assess the function of LbPMEs during ECM formation, we altered the LbPME transcript levels in *L. bicolor* through RNAi or overexpression constructs driven by the constitutive *Agaricus bisporus gpdII* promoter (Fig. S1). For RNAi silencing, the promoter was followed either by a hairpin construct generating siRNAs against *LbPME1* (*LbPME1*-RNAi) or a combined hairpin construct generating siRNAs against *LbPME1* and all three other PMEs that are closely related in sequence (*LbPME1-4*-double RNAi, Figs S1, S17). In FLM of the three selected *LbPME1-4*-double RNAi lines, the levels of all four LbPMEs were significantly reduced by 60% compared with levels in wild-type FLM (Figs 4a, S2). In the three selected single RNAi lines, specifically *LbPME1* expression but not *LbPME2-4* was reduced to a similar extent, as in the double-RNAi lines. Finally, in the three selected *LbPME1* overexpressor lines, *LbPME1* transcript levels were increased by 4.9–7.9-fold compared with wild-type FLM, whilst no effect was observed on transcript levels of the other LbPMEs (Figs 4b, S2). We also assessed the expression level of the three ECM-induced LbPGs (Fig. S6) in FLM. *LbPG* JGI ID #388191 was not detected with two different primer pairs, *LbPG2* (JGI ID #612983), and *PbPG1* (JGI ID #613299, *LbGH28A* in Zhang *et al.* (2022)) did not show any significant

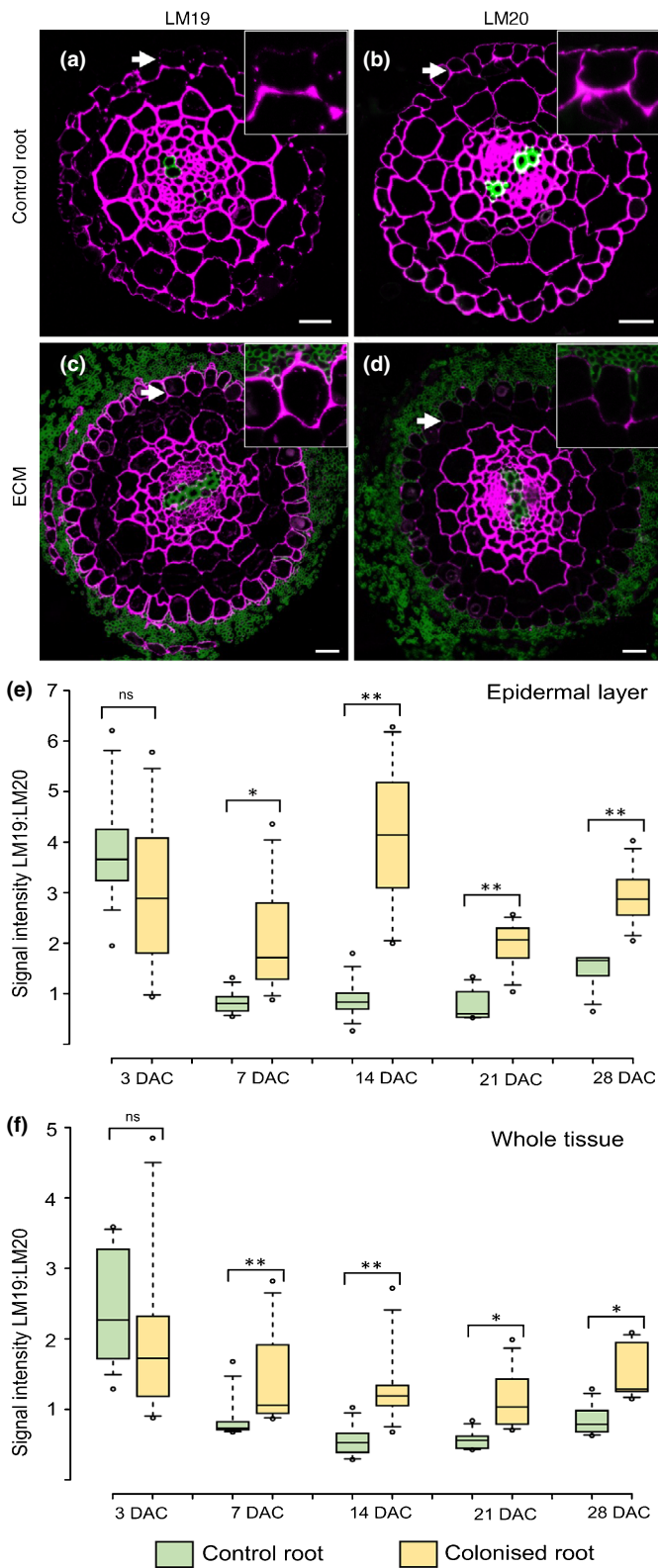


Fig. 3 Immunolocalisation with pectin antibodies LM19 (recognising de-esterified homogalacturonan (HG) (a, c) and LM20 (recognising methylesterified HG (b, d) in 1- μ m thin cross-sections of control roots without fungus (a, b) and colonised roots (c, d) collected at 14 d after contact (DAC) (or control without fungus). *Laccaria bicolor* is visualised by labelling with WGA-AF488 (green); and plant cell-wall homogalacturonan is visualised with LM19 and LM20 antibody conjugated Cy5 (magenta). White arrows indicate the epidermal layer where the difference of antibody labelling abundance is evident between ectomycorrhiza (ECM) and control roots. Bars, 20 μ m. Insets in (a–d) show a magnified view of three adjacent epidermal cells. Boxplots showing the fluorescence intensity ratio of LM19 and LM20 in the epidermal layer (e) and whole tissue area (f), respectively, at the indicated time points after contact. Data were collected from 10 observations per root and four or five roots per time point and condition. Boxes indicate the interquartile range (25th to 75th percentile), the horizontal line inside the box marks the median, whiskers show minimum and maximum values and circles mark outliers. ns, nonsignificant; **, $P < 0.01$; *, $P < 0.05$; using Student's *t*-test.

expression patterns observed across all samples (Fig. S18). In line with LbPME expression results, PME activity assays on FLM grown on P20 supplemented with freeze-dried root cell-wall powder indicated significant reductions of LbPME activity in all *LbPME1* RNAi and *LbPME1-4* double RNAi lines (Fig. 4c). Conversely, two of our three overexpressor lines showed significantly increased LbPME activity. However, there was no strong correlation between transcript levels and PME activity levels inside mycelia samples (Fig. S19), which may be due to secretory loss of PME from the mycelium into the growth media. We selected the lines that had both confirmed altered LbPME transcript and activity levels for further characterisation. To test whether altered PME activity affects the fungal ability to utilise pectin as a carbon source, we grew transgenic lines in modified P20 medium containing pectin that was highly methylesterified or unesterified as the only carbon source. Whilst on P20 (with glucose as carbon source) none of the transgenic lines showed a significant difference in growth compared with control lines, their growth was significantly reduced in both types of pectin-containing media, irrespective of whether *LbPME* levels had been upregulated or downregulated (Fig. 5). In these pectin media, the hindered growth of PME RNAi lines with restricted PME activity was expected, as it suggests that RNAi lines have a reduced ability to utilise pectin. The hampered growth of the overexpressor lines was unexpected.

Transgenic alteration of *LbPMEs* alters ECM formation and depth of Hartig net

To assess the role of LbPMEs in ECM development, we performed interaction assays between the selected *L. bicolor* lines and *P. tremula* \times *P. tremuloides* and analysed root phenotypes at 14 DAC, which is the earliest time point when ECM can be distinguished well visually and the Hartig Nets are detected in sectioned material (Fig. S3). Depending on the individual line, we found a 22–51% decrease in the number of swollen ECM roots with visible mycelia attachment (Fig. S20) in interactions with *LbPME1* RNAi lines and *LbPME1-4* double RNAi lines (Fig. 6). Unexpectedly, both selected *LbPME1* overexpressor

alteration except for a slight induction of both genes in *LbPME1* RNAi line 31 (Fig. S18). As the transcript sequences or *LbPG1* and *LbPG2* are 94% identical, we may however observe cross-hybridisation of primers, indicated by the similar

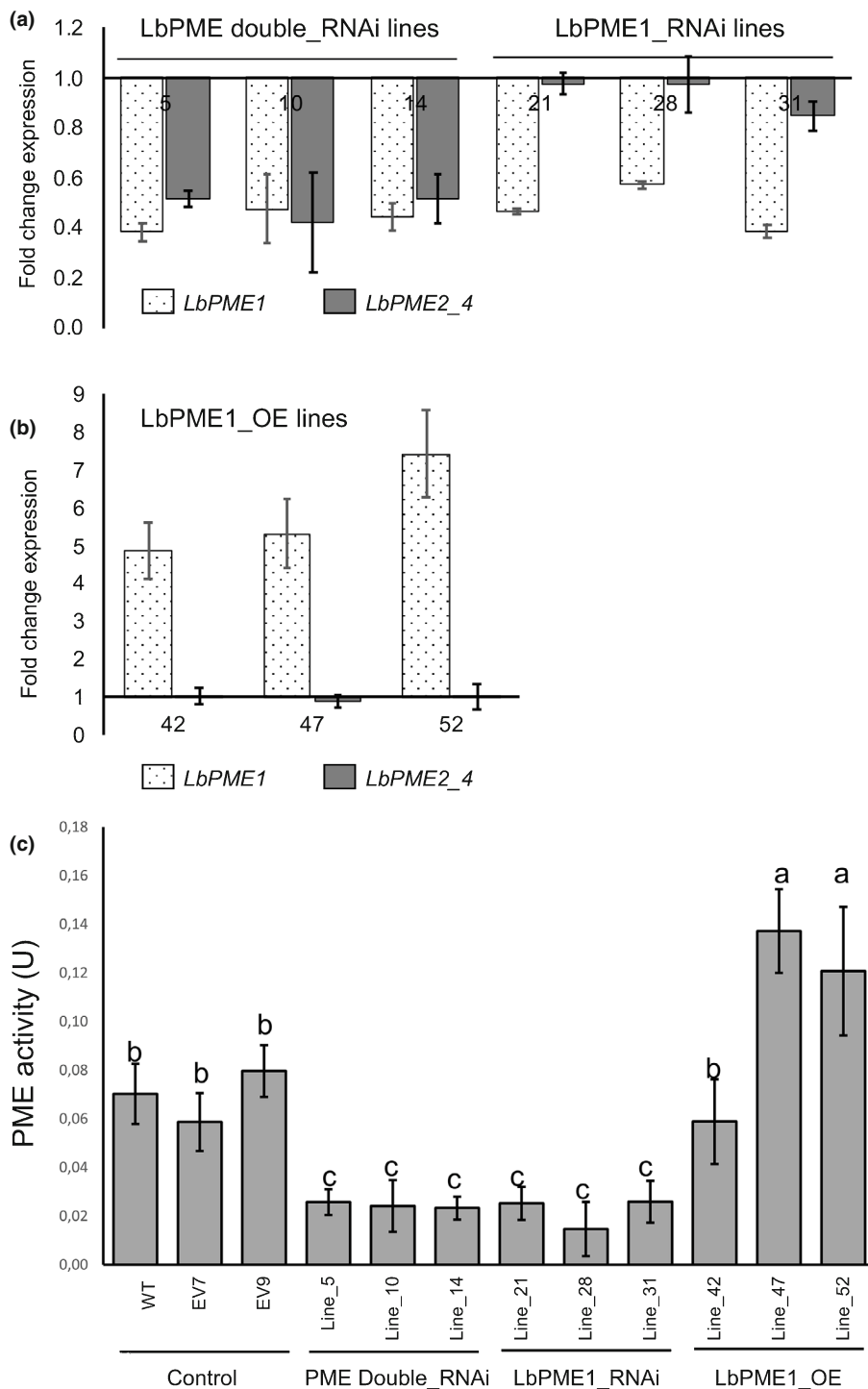


Fig. 4 Relative normalised expression of *Laccaria bicolor* pectin methylesterase (PME) transcripts in free-living mycelia of the selected transgenic fungal lines (indicated by number) at 14 d of growth compared with wild-type control (a, b). Error bars indicate standard error of the mean. PME activity in the free-living mycelia of transgenic *L. bicolor* lines grown on modified P20 medium containing powdered poplar root cell wall (c). PME activity was measured as the milli-unit when one unit released 1.0 micro-equivalent of acid from pectin per min at pH 7.5 at 30°C. EV7 and EV9 refer to empty vector (EV) mock transformant lines. Statistical analysis was performed using Fisher's least significant difference (LSD) test. The PME activity differences in transgenic fungal lines marked with different letters are statistically significant. Error bars indicate standard deviation.

lines showed reduced ECM frequency comparable with the RNAi lines.

To confirm the results from morphological observations, we assessed the expression of symbiosis-associated marker genes – two previously characterised from *L. bicolor* and one from *Populus* – in RNA from randomly collected lateral roots at 14 DAC (containing noncolonised, colonised and ECM roots) in interactions with the transgenic *L. bicolor* lines: *PF6.2* (JGI ID

#469385) (Kim *et al.*, 1998; Podila *et al.*, 2002; Hiremath *et al.*, 2013), *Aquaporin* (JGI ID #671860) (Dietz *et al.*, 2011; Kohler *et al.*, 2015) and the sugar transporter *PtSWEET1* (Neb *et al.*, 2017). We confirmed that these genes were induced in co-cultures with control (empty vector) *L. bicolor* lines compared with conditions in which both organisms were grown separately (Fig. 7a,b). Consistent with morphological observations, *PF6.2*, *Aquaporin* and *PtSWEET1* were significantly downregulated in

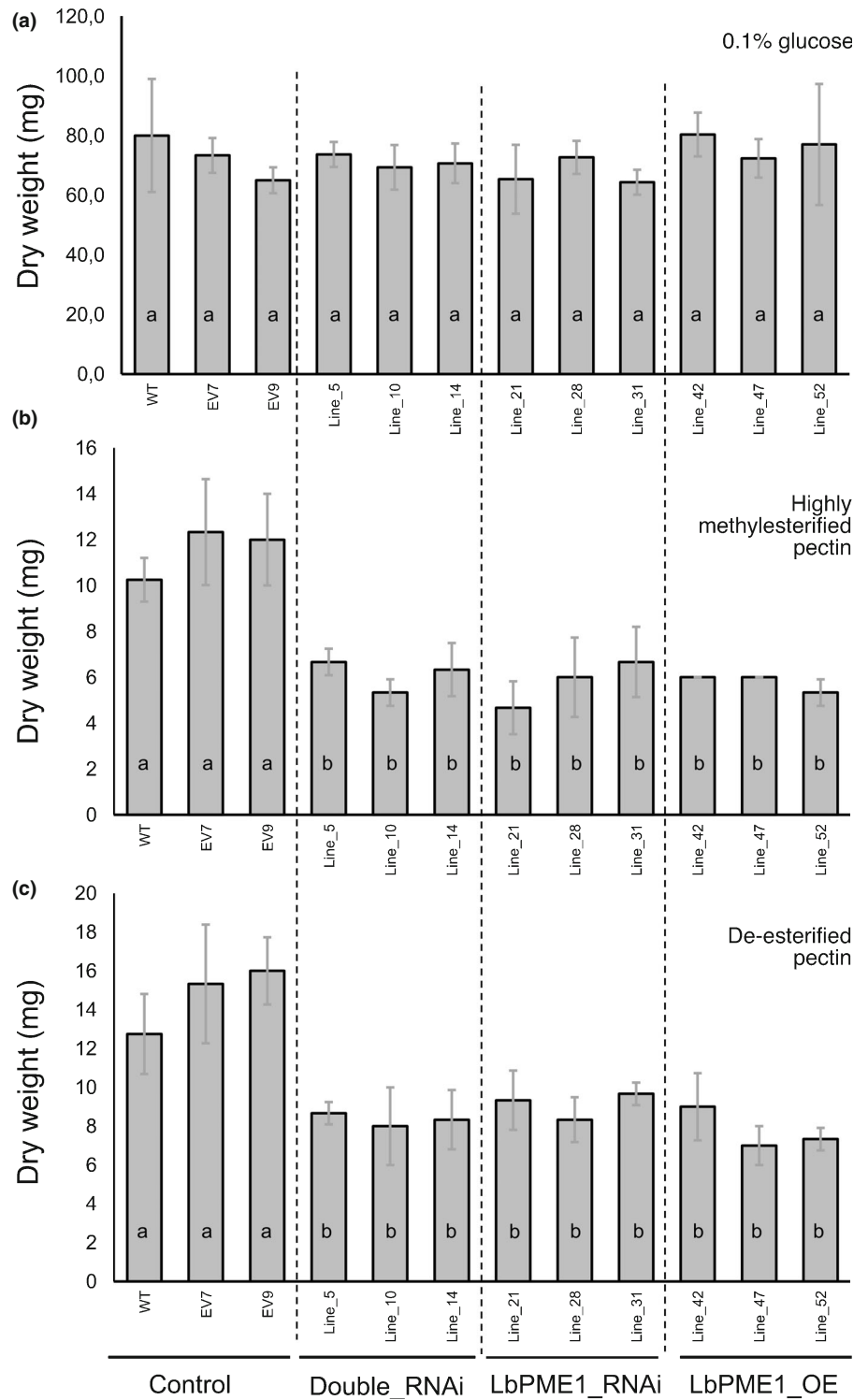


Fig. 5 Growth of free-living mycelia of *LbPME* transgenic lines in medium containing various sources of carbon. Media include conventional P20 with 0.1% glucose (a), modified P20 with highly methylesterified pectin (b) and with de-esterified pectin (c) as the carbon source. Growth was measured on a dry weight basis. Error bars indicate standard deviation. Significant differences among samples are indicated by unique letters according to Fisher's least significant difference (LSD) ANOVA test (P -value ≤ 0.05).

co-cultures with the RNAi and overexpressor lines compared with co-cultures with empty vector control lines at 14 DAC (Fig. 7c–e). With this experiment we also confirmed that *LbPME1* transcript levels in all selected overexpressor and RNAi lines were altered similarly in free-living mycelium (Fig. 4a) and in mycelium in contact with roots (Fig. 7f). Finally, we examined expression levels of ECM-induced LbPGs (using the primer for JGI ID #612983 that was likely to also recognise ID #613299,

LbGH28A) as changes in PME expression levels may affect the expression of the HG-degrading PGs (Hadfield & Bennett, 1998). Although there was no alteration of PG expression in the FLM of PME altered lines (Fig. S15), we found a significant reduction of LbPG transcript levels in co-cultures with RNAi and OE lines compared with co-cultures with control *L. bicolor* lines (Fig. 7g). This suggests that PG-mediated HG depolymerisation may be reduced in co-cultures with RNAi and OE lines.

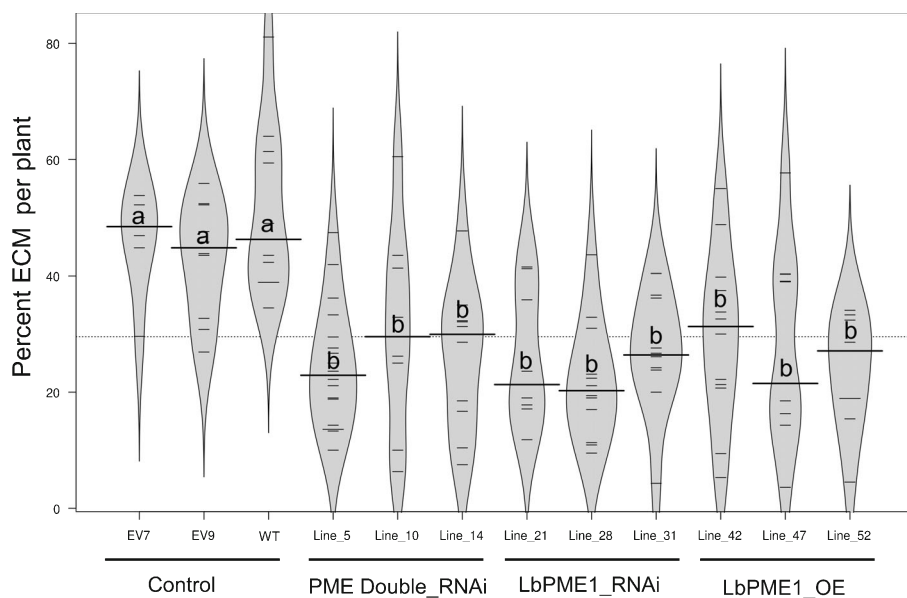


Fig. 6 Bean plot showing the frequency of *Populus tremula* × *Populus tremuloides* ectomycorrhiza (ECM) at 14 d after contact (DAC) with wild-type or genetically modified *Laccaria bicolor* lines. The width of each column indicates the density of observations and the short horizontal lines represent ECM number per observed plant. Long horizontal lines indicate the mean value. Significant differences among samples are indicated by unique letters according to Fisher's least significant difference (LSD) ANOVA test (P -value ≤ 0.05).

We furthermore measured the depths and areas of Hartig Nets in cross-sections of ECM with the RNAi and OE lines compared with ECM with wild-type *L. bicolor*. As micrographs revealed, Hartig net depths in ECM with the RNAi lines were reduced by 60% compared with ECM with wild-type fungus (Figs 8a, S21c, d). This suggested that the reduced PME activity restricted the ability of the RNAi lines to loosen plant cell walls and to induce root cell separation by the RNAi lines. ECM with *LbPME1* OE lines, by contrast, produced slightly deeper Hartig Nets (on average 18% deeper than wild-type) (Figs 8a, S21e). The expression of *LbPMEs* also affected the Hartig net area in between adjacent root cells representing the colonised area in the apoplastic region (Fig. 8b). Depending on the lines, the area was reduced by *c.* 40% among the RNAi lines and increased by *c.* 40% among the OE lines. Using LM19 antibodies to detect de-esterified HG in ECM cross-sections at 14 DAC, we detected reduced labelling in radial epidermal walls of ECM with RNAi lines (significant at $P < 0.05$ for *LbPME* double RNAi lines, visible trend for *LbPME1* single RNAi lines; $P = 0.067$) compared with ECM with control lines or *LbPME* OE lines, despite the variation between the individual lines (Fig. S21f). Taken together, these results showed that *L. bicolor* requires an optimal PME level to form ECM, whereas sub-optimal *LbPME* expression, whether reduced or increased, negatively affected ECM frequency. Whilst the transgenic reduction of *LbPME* expression lowered cell-wall de-esterification, Hartig net depth and ECM frequency, increased *LbPME* levels did not increase ECM frequency nor de-esterification in the epidermal layer, but resulted in a deeper Hartig net.

Discussion

The molecular mechanisms of cell-wall remodelling associated with ECM development are just beginning to be understood despite their importance for Hartig net formation (Balestrini & Bonfante, 2014). As revealed using whole-genome sequences,

most ECM fungi have a reduced set of PCWDEs compared with their saprotrophic ancestors. The loss of PCWDEs has been suggested to be the result of potential mechanisms to avoid pattern triggered immunity responses from host plants and to make colonisation possible. Nevertheless, from the transcriptome analyses of various ECM interactions, including our present, it is evident that ECM-specific induction of PCWDEs commonly occurs, and is likely to be necessary for ECM formation (Sebastian *et al.*, 2014; Veneault-Fourrey *et al.*, 2014; Kohler *et al.*, 2015). A recent study has shown that ECM formation requires the *L. bicolor* endoglucanase *LbGH5-CBM* to act on plant cell-wall cellulose. Silencing of this gene reduced *L. bicolor*'s ability to form ECM (Zhang *et al.*, 2018). Like cellulose, HG is a major component of the plant cell wall, although it is mainly localised in the middle lamella. HG is considered a key polymer for cell-to-cell adhesion (Bouton *et al.*, 2002; Daher & Braybrook, 2015) and our study, together with another recent report (Zhang *et al.*, 2022), revealed that the modulation of the HG-rich middle lamella is a prerequisite for complete Hartig net formation and entails the action of members of two families of *L. bicolor* HGMEs.

The increased abundance of de-esterified HG, especially in the area in which the Hartig net actively forms from 7 DAC onwards (Fig. 3), is in line with a previous study that, using JIM5 antibody labelling, demonstrated the presence of de-esterified HG epitopes in the proximity of the Hartig net in *Tuber melanosporum* and *Corylus avellana* ECM (Sillo *et al.*, 2016). However, Sillo *et al.* (2016) reported also that, using a carbohydrate microarray, all HG epitopes along with other PCW polysaccharides significantly decreased in ECM with *T. melanosporum* compared with noncolonised root tissues of *C. avellana*. This discrepancy is most probably due to the different nature of the materials used in this study. Only the plant partner contains HG; therefore, when bulk material from roots and ECM (root and fungus) are extracted and compared, and

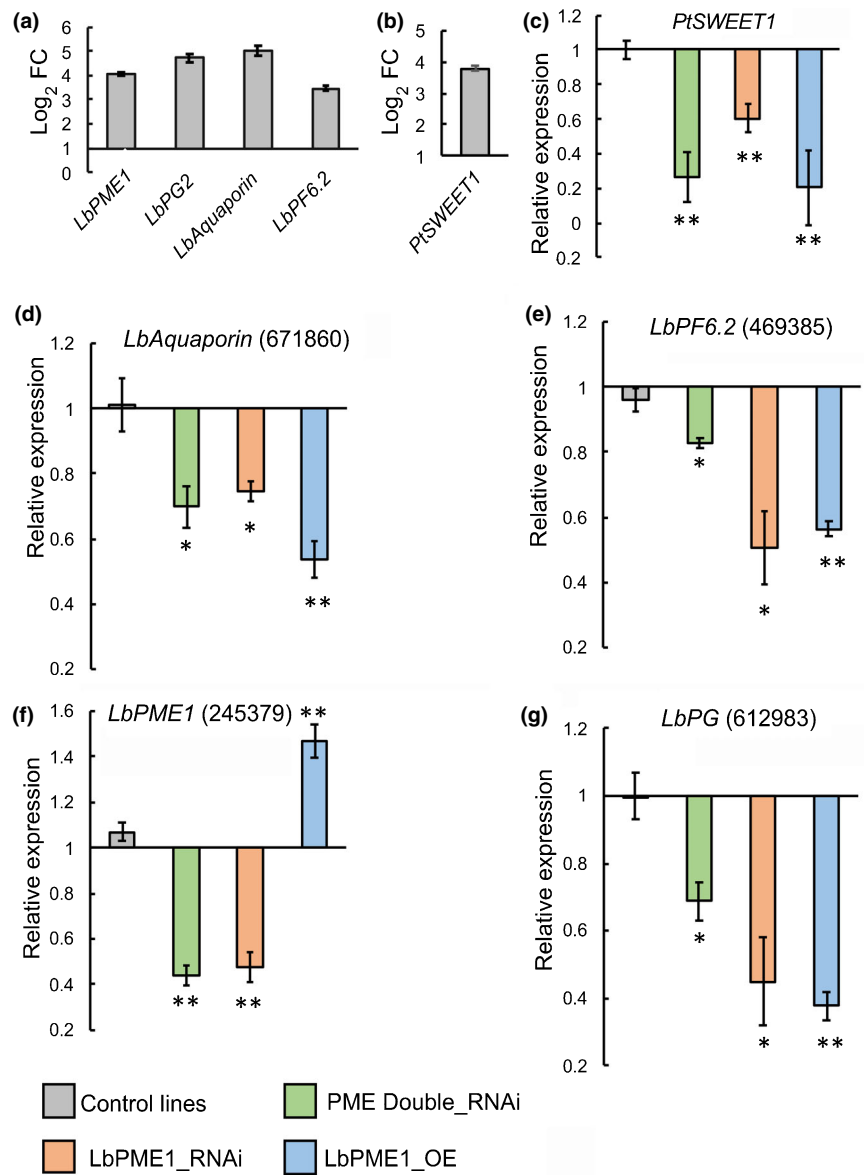


Fig. 7 Relative normalised expression of selected homogalacturonan modifying genes (HGMEs) and ectomycorrhiza-related genes of *Laccaria bicolor* and *Populus* in co-culture tissue (comprising ectomycorrhiza (ECM), colonised roots and noncolonised roots) at 14 d after contact (DAC) determined using qPCR. Log₂ fold induction of the gene of interests in control *L. bicolor* (average of wild-type and mock vector control lines) interacting with *Populus tremula* × *Populus tremuloides* (14 DAC) relative to free-living mycelia without the plant (a), or ectomycorrhizal *P. tremula* × *P. tremuloides* roots in interaction wild-type and empty vector *L. bicolor* lines (14 DAC) relative to noncolonised roots (b). Fold change of genes of interest in co-cultures with the transgenic lines relative to co-cultures with control lines of *L. bicolor* (c–g). For each construct, co-culture samples with the three selected transgenic *L. bicolor* lines were considered as three biological replicates. Expression of each gene was normalised against their expression in wild-type *L. bicolor*–*P. tremula* × *P. tremuloides* interaction. Student's *t*-test: **, *P* < 0.01; *, *P* < 0.05 compared with wild-type. Error bars indicate the standard error of the mean.

the results from ECM are normalised on total ECM weight, one can expect to detect a reduced (diluted) amount of HG in extracts from ECM roots, regardless of the methylesterification state per se. Therefore, we took advantage of quantitative immunofluorescence microscopy to assess the HG methylesterification state at the tissue level. To normalise for root-to-root variation of HG methylesterification, we compared roots and ECM of similar age at specific time points, by measuring the signal intensity ratio arising from LM19 and LM20 epitopes (Fig. 3). From this we could deduce the proportion of de-esterified and highly methylesterified HG in the ECM composite material. The HG de-esterification pattern during the interaction of *Populus* with *L. bicolor* resembled several other plant interactions with fungal root pathogens, that is pectin is de-esterified by PMEs to make tissues more vulnerable to pathogen CWDEs (Lionetti *et al.*, 2012; Ma *et al.*, 2013; Fan *et al.*, 2017). Our finding of increased HG de-esterification

during Hartig net formation is consistent with our further observation that PME activity is increased in ECM roots. Even though it is not possible to conclude from this experiment whether it is the plant or the fungal partner, or both, that exerts the enhanced activity in ECM tissues, our further analyses support the importance of fungal LbPMEs in the process.

PMEs are the key enzymes controlling the HG methylesterification status, whereas galacturonosyl transferase or pectin methyltransferase activity does not affect the methylesterification degree of HG (Mouille *et al.*, 2007; Wolf *et al.*, 2009). However, given our current state of knowledge, we only partly understand the action and consequences of PME-mediated HG de-esterification. It may either lead to cell-wall loosening by PGs and PLs, or it may cause cell-wall rigidification through calcium cross-linking and the formation of the so-called egg box (Sénéchal *et al.*, 2014; Hocq *et al.*, 2017; Wormit & Usadel, 2018). Specific physiological conditions may determine this fate.

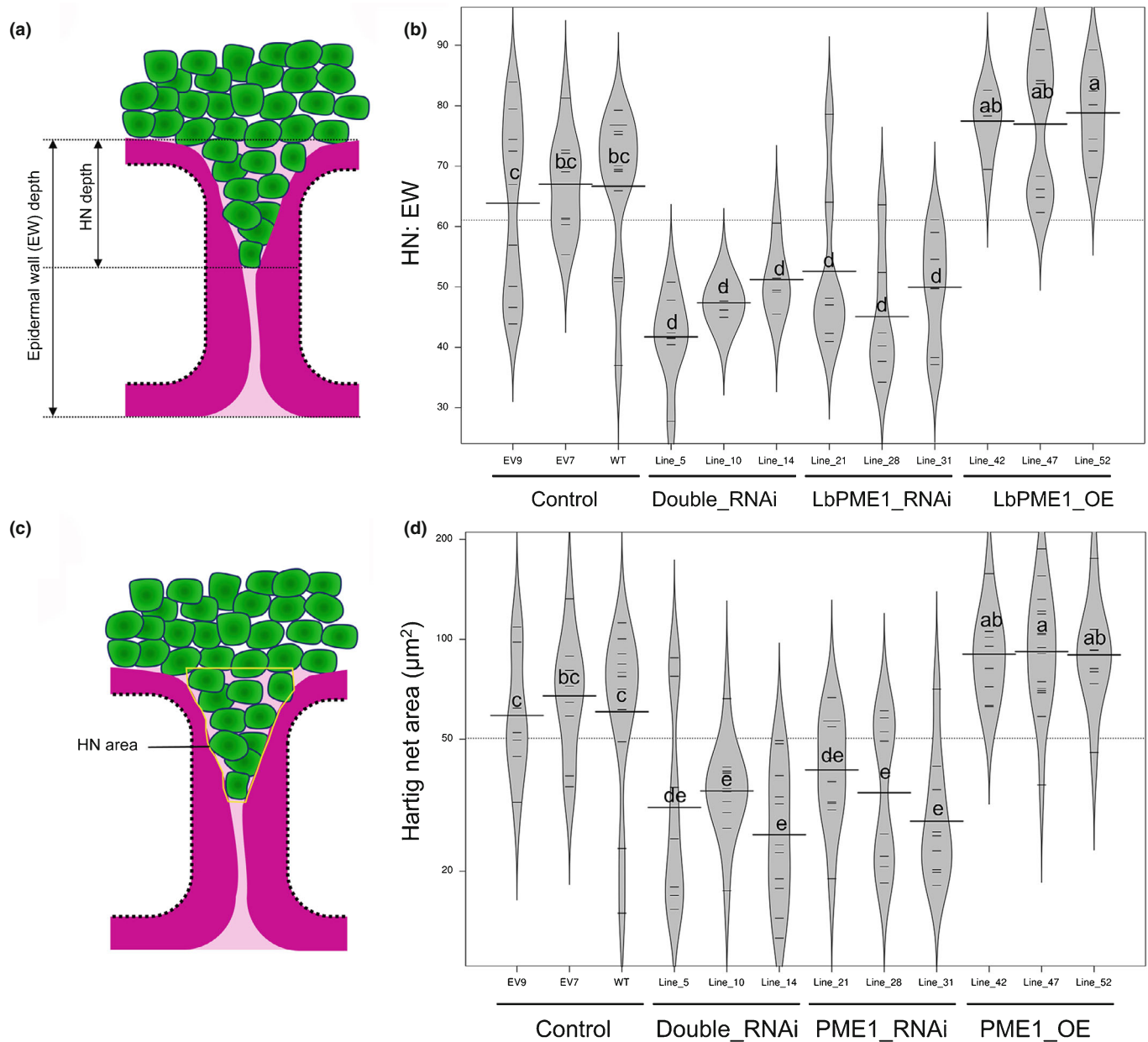


Fig. 8 Hartig net (HN) depth and area in *Populus tremula* × *Populus tremuloides* ectomycorrhiza (ECM) at 14 d after contact (DAC) with wild-type or genetically modified *Laccaria bicolor*. HN depth is represented as the percentage of the area of the radial epidermal wall (EW) covered by *L. bicolor* (a). Bean plot showing HN depth as the ratio of HN and EW among various interactions (b). The HN area represents the area of fungal hyphae between epidermal cells (c). Bean plot showing the ratio of HN and EW among various interactions (d). Whilst long horizontal lines indicate the mean value, small horizontal lines represent individual data points and polygons represent the estimated density of the data (b, d). Significant differences among lines are indicated by unique letters according to Fisher's least significant difference (LSD) ANOVA test (P -value ≤ 0.05).

We assume that PME-mediated HG de-esterification throughout ECM development leads rather to HG degradation and cell-wall loosening. This argument is supported by a significant induction of three fungal PGs and one plant PG potentially catalysing HG depolymerisation in ECM, and advocates for HG breakdown during ECM formation. Furthermore, recent evidence has proved that the fungal polygalacturonase LbGH28A indeed acts on pectin (Zhang *et al.*, 2022). LbGH28A could be a probable actor downstream of the action of LbPME, in which LbPME1 catalyses HG de-esterification and LbGH28A breaks down the

de-esterified HG. As *L. bicolor* only possesses these two types of pectin-related enzyme families (Veneault-Fourrey *et al.*, 2014), further catalytic functions may be carried out by plant enzymes (Figs S7, S22) during the earlier stages of ECM formation. Three plant PMEs were upregulated up to the 14 DAC time point but thereafter we only observed downregulation of plant PMEs (Fig. S7). The product of the two plant *PMEs* induced at 21 DAC may inhibit any remaining expressed plant PMEs (Juge, 2006; Pelloux *et al.*, 2007; Sénéchal *et al.*, 2014; Wormit & Usadel, 2018). Plant PMEs do not, however, seem to be

capable of inhibiting fungal and bacterial PME activity due to the absence of critical residues for PME–PMEI interactions in microbial PMEs (Di Matteo *et al.*, 2005; Lionetti *et al.*, 2007; Reça *et al.*, 2012) including LbPMEs (Fig. S10). The significant upregulation of *LbPME1* throughout the different stages of ECM development that precedes detectable de-esterification (from 7 DAC), and its potential insensitivity to PMEI-mediated inhibition, led us to consider this gene as a potential key contributor to HG de-esterification. *LbPME1* is also the only PME induced in the interaction with other tree species, namely *Populus trichocarpa* and *Pseudotsuga menziesii* (Plett *et al.*, 2015). This suggests that *LbPME1* is an ECM-associated fungal PME isoform potentially regulating cell-wall remodelling during Hartig net formation.

Our functional approach using single and double LbPME RNAi lines showed that the ECM-induced *LbPME1* is not functionally redundant to *LbPME2* to *LbPME4*, that is suppression of *LbPME1* did not induce other LbPME members (Fig. 4a,b), nor did other LbPMEs compensate functionally for LbPME repression. The latter was supported by our finding that PME activity of single RNAi and double RNAi lines did not significantly differ (Fig. 4c), and that the double RNAi construct did not cause additional phenotypes compared with the single RNAi construct (Figs 6, 8). The fact that LM19 signals were reduced at the 95% significance level only in the double RNAi but not the single RNAi lines despite a visible trend, can be attributed to variations between the individual lines (Fig. S21f). As we observed the expected increased PME activity in *L. bicolor* lines overexpressing LbPME1 and decreased PME activity in RNAi lines (Fig. 4c), we deemed *in vitro* enzyme characterisation of *LbPME1* unnecessary.

The fact that RNAi lines had a lower ECM frequency, reduced Hartig net depth and a decreased expression level of marker genes, suggests that HG de-esterification, with the contribution of *L. bicolor* *LbPME1*, is needed for full Hartig net formation. This also supports the idea that this step is a prerequisite for enzymatic breakdown of HG polymers by PGs and PLs (Verlent *et al.*, 2005), with potential contribution by LbGH28 (Zhang *et al.*, 2022). Strikingly, although OE lines had significantly increased Hartig net depth and area (Fig. 8) in roots that managed to form ECM with this line, overall ECM frequency was decreased in the same way as in RNAi lines, as was a marker for gene expression. Furthermore, the expression of an ECM-induced polygalacturonase gene, *LbPG2*, was significantly reduced in colonised roots with all transgenic lines when compared with roots colonised by the wild-type fungus (Fig. 7), which indicated a correlation with reduced HG breakdown and ECM formation. One could hypothesise that the overproduction of LbPME1 in the OE lines leads to blockwise de-esterification of HG, which creates potential binding sites for Ca^{2+} and egg-box formation (Cabrera *et al.*, 2008), thereby stiffening the middle lamella and reducing the access of depolymerising enzymes such as PGs and PLs for HG breakdown (Ralet *et al.*, 2001; Pelloux *et al.*, 2007; Ngouémazong *et al.*, 2012; Sénéchal *et al.*, 2014). However, we estimated that this scenario was rather unlikely, as the existence of egg-box

structures *in planta* has recently been questioned and atomic force microscopy suggested that overexpression of PME resulted in a reduced stiffness of cell walls (Hocq *et al.*, 2017). Nevertheless, these structures may have been formed in the growth experiments of FLM on plates with pectin as a carbon source (Fig. 5). Under those conditions, it is possible that an overproduction of LbPME by the OE lines led to blockwise de-esterification of HG that acts as a nucleation site of ions such as Mg^{2+} , abundant in the growth medium. Formation of these metal ion bridges may hinder degradation of HG by the activity of PGs (Sénéchal *et al.*, 2014) and thereby reduce the availability of carbon from the pectin for fungal nutrition. This would then result in reduced growth even in the overexpressor lines, as observed and expected in RNAi lines that have a reduced capacity to make carbon available from HG present in the media.

Concerning the *in planta* scenario during ECM formation, which would explain reduced ECM frequency in plants in contact with *LbPME1* overexpressor lines, it is likely that PME overproduction triggers excessive HG degradation involving PGs or PLs. This would then result in an enhanced release of oligogalacturonides (OGs) triggering OG-induced systemic defence responses that could counteract ECM formation. In support of this, several studies have provided evidence that OGs, upon binding to wall-associated kinases (WAKs), elicit defence responses, including the induction of pathogenesis-related proteins and reactive oxygen species (Anderson *et al.*, 2001; Decreux & Messiaen, 2005; Ferrari *et al.*, 2013; Benedetti *et al.*, 2015). During plant invasion by pathogens, binding of OGs to WAKs triggers MAPK-mediated activation of OG-specific defence gene expression that is independent of salicylic acid-, jasmonic acid- and ethylene-mediated signalling pathways (Ferrari *et al.*, 2007; Chasot *et al.*, 2008). Even though overall ECM formation with the overexpressor lines may be restricted by such a systemic *in planta* defence response, at the few positions in which ECM manage to form, the enhanced PME activity would lead to deeper Hartig net formation. Even though we did not detect a higher abundance of LM19 epitopes in radial epidermal walls in ECM with LbPME1 overexpressors at the 14 DAC time point (Fig. S21f), the deeper Hartig net and larger Hartig net area could indicate a quicker progression of Hartig net formation, resulting in a more advanced stage at the time point of observation (Fig. S3). This scenario would be in line with a more strongly triggered defence response in roots as hypothesised previously. This hypothesis and the signalling pathways behind it will need to be verified experimentally in the future.

In conclusion, HG de-esterification of the host cell wall is a critical step for cell-wall remodelling and Hartig net formation during the *L. bicolor* and *P. tremula* × *P. tremuloides* interaction. The fungal pectin methylesterase *LbPME1* is essential in this process. LbPME1 may play a similar role for the interactions of *L. bicolor* with other *Populus* species and *Pseudotsuga menziesii* because of their expression similarities (Plett *et al.*, 2015). Even though ECM fungi may have retained only a small repertoire of pectin-related CAZymes (Kohler *et al.*, 2015; Martin *et al.*, 2016; Miyauchi *et al.*, 2020), the reduced machinery in *L.*

bicolor makes a significant contribution to ECM formation. Despite the wide retention of the machinery in fungi with different lifestyles, we know a few ECM fungi that lack *CE8* (PME) and/or *GH28* genes (Kohler *et al.*, 2015; Miyachi *et al.*, 2020). It will be interesting to explore in future studies the mechanisms of pectin remodelling in relationships with fungi that lack the mechanism described here.






Acknowledgements

JC was supported by the Kempe Foundations (SMK-1533) and by Formas, a Swedish Research Council for Sustainable Development (942 2105-539). Funding to MK and AGP was provided by grants from the National University of Quilmes (UNQ), National Council of Scientific and Technical Research (CONICET), and National Agency for Scientific and Technological Promotion (ANPCyT), Argentina. We would like to acknowledge support from Science for Life Laboratory, the National Genomics Infrastructure funded by the Swedish Research Council, and Uppsala Multidisciplinary Center for Advanced Computational Science for assistance with massively parallel sequencing and access to the UPPMAX computational infrastructure. The authors acknowledge the facilities and technical assistance of the Biopolymer Analytical Platform (BAP) at SLU/KBC, Umeå University and the Umeå Core Facility Electron Microscopy (UCEM) at the Chemical Biological Center (KBC), Umeå University. The authors acknowledge the facilities and technical assistance of the Umeå Plant Science Centre (UPSC) Microscopy Facility.

Author contributions

JC and JL-F designed the study, JC conducted and analysed the experiments. MK designed constructs for transgenic lines used in this project, and prepared and transformed *L. bicolor* under AGP's supervision. ND and IS performed bioinformatics analysis. JZ carried out insert number and site characterisation of transgenic *L. bicolor* lines. JT was involved in setting up PME activity assays. JL-F supervised the study. JC and JL-F wrote the manuscript with contribution of all authors.

ORCID

Jamil Chowdhury  <https://orcid.org/0000-0002-1113-3496>
 Nicolas Delhomme  <https://orcid.org/0000-0002-3053-0796>
 Minna Kempainen  <https://orcid.org/0000-0002-4240-4690>
 Judith Lundberg-Felten  <https://orcid.org/0000-0002-0444-822X>
 Junko Takahashi  <https://orcid.org/0000-0003-1818-3768>

Data availability

The raw transcriptomics data are available from the European Nucleotide Archive (ENA, <https://ebi.ac.uk/ena>) under the accession no. PRJEB41173. A GIT-Hub repository of data analysis

performed is available under doi: [10.5281/zenodo.4629643](https://doi.org/10.5281/zenodo.4629643) at <https://doi.org/10.5281/zenodo.4629643> while the code is available at <https://github.com/nicolasDelhomme/laccariaBicolorEcmDev/tree/v1.0>.

References

- Abras KAL, Bilger I, Martin F, Tacon F. 1988. Morphological and physiological changes in ectomycorrhizas of spruce [*Picea excelsa* (Lam.) Link] associated with ageing. *New Phytologist* 110: 535–540.
- Anderson CM, Wagner TA, Perret M, He ZH, He D, Kohorn BD. 2001. WAKs: cell wall-associated kinases linking the cytoplasm to the extracellular matrix. *Plant Molecular Biology* 47: 197–206.
- Anderson CT, Carroll A, Akhmetova L, Somerville C. 2010. Real-time imaging of cellulose reorientation during cell wall expansion in Arabidopsis roots. *Plant Physiology* 152: 787–796.
- Anthorn GE, Barrett DM. 2004. Comparison of three colorimetric reagents in the determination of methanol with alcohol oxidase. Application to the assay of pectin methyltransferase. *Journal of Agricultural and Food Chemistry* 52: 3749–3753.
- Balestrini R, Bonfante P. 2014. Cell wall remodeling in mycorrhizal symbiosis: a way towards biotrophism. *Frontiers in Plant Science* 5: 237.
- Balestrini R, Hahn MG, Bonfante P. 1996. Location of cell-wall components in ectomycorrhizae of *Corylus avellana* and *Tuber magnatum*. *Protoplasma* 191: 55–69.
- Benedetti M, Leggio C, Federici L, De Lorenzo G, Pavel NV, Cervone F. 2011. Structural resolution of the complex between a fungal polygalacturonase and a plant polygalacturonase-inhibiting protein by small-angle X-ray scattering. *Plant Physiology* 157: 599–607.
- Benedetti M, Pontiggia D, Raggi S, Cheng Z, Scaloni F, Ferrari S, Ausubel FM, Cervone F, De Lorenzo G. 2015. Plant immunity triggered by engineered in vivo release of oligogalacturonides, damage-associated molecular patterns. *Proceedings of the National Academy of Sciences, USA* 112: 5533–5538.
- Bidhendi AJ, Geitmann A. 2016. Relating the mechanics of the primary plant cell wall to morphogenesis. *Journal of Experimental Botany* 67: 449–461.
- Bonfante P, Genre A. 2010. Mechanisms underlying beneficial plant-fungus interactions in mycorrhizal symbiosis. *Nature Communications* 1: 48.
- Bouton S, Leboeuf E, Mouille G, Leydecker M-T, Talbot J, Granier F, Lahaye M, Höfte H, Truong H-N. 2002. QUASIMODO1 encodes a putative membrane-bound glycosyltransferase required for normal pectin synthesis and cell adhesion in Arabidopsis. *Plant Cell* 14: 2577–2590.
- Brundrett M. 2004. Diversity and classification of mycorrhizal associations. *Biological Reviews of the Cambridge Philosophical Society* 79: 473–495.
- Burton RA, Collins HM, Kibble NAJ, Smith JA, Shirley NJ, Jobling SA, Henderson M, Singh RR, Pettolino F, Wilson SM *et al.* 2011. Over-expression of specific *HvCslF* cellulose synthase-like genes in transgenic barley increases the levels of cell wall (1,3;1,4)- β -d-glucans and alters their fine structure. *Plant Biotechnology Journal* 9: 117–135.
- Cabrera JC, Boland A, Messiaen J, Cambier P, Van Cutsem P. 2008. Egg box conformation of oligogalacturonides: the time-dependent stabilization of the elicitor-active conformation increases its biological activity. *Glycobiology* 18: 473–482.
- Catoire L, Pierron M, Morvan C, du Penhoat CH, Goldberg R. 1998. Investigation of the action patterns of pectinmethyltransferase isoforms through kinetic analyses and NMR spectroscopy. Implications in cell wall expansion. *The Journal of Biological Chemistry* 273: 33150–33156.
- Chassot C, Buchala A, Schoonbeek H-J, Métraux J-P, Lamotte O. 2008. Wounding of Arabidopsis leaves causes a powerful but transient protection against *Botrytis* infection. *The Plant Journal* 55: 555–567.
- Chowdhury J, Henderson M, Schweizer P, Burton RA, Fincher GB, Little A. 2014. Differential accumulation of callose, arabinoxylan and cellulose in nonpenetrated versus penetrated papillae on leaves of barley infected with *Blumeria graminis* f. sp. *hordei*. *New Phytologist* 204: 650–660.
- Daher FB, Braybrook SA. 2015. How to let go: pectin and plant cell adhesion. *Frontiers in Plant Science* 6: 523.

- Decreux A, Messiaen J. 2005. Wall-associated kinase WAK1 interacts with cell wall pectins in a calcium-induced conformation. *Plant & Cell Physiology* 46: 268–278.
- Delhomme N, Mähler N, Schifffhaller B, Sundell D, Mannapperuma C, Hvidsten TR, Street N. 2014. *Guidelines for RNA-Seq data analysis*. Epigenesis. [WWW document] URL https://www.epigenesis.eu/images/stories/protocols/pdf/20150303161357_p67.pdf [accessed 12 June 2019].
- Denès JM, Baron A, Renard CM, Péan C, Drilleau JF. 2000. Different action patterns for apple pectin methyltransferase at pH 7.0 and 4.5. *Carbohydrate Research* 327: 385–393.
- Di Matteo A, Giovane A, Raiola A, Camardella L, Bonivento D, De Lorenzo G, Cervone F, Bellincampi D, Tsernoglou D. 2005. Structural basis for the interaction between pectin methyltransferase and a specific inhibitor protein. *Plant Cell* 17: 849–858.
- Dietz S, von Bülow J, Beitz E, Nehls U. 2011. The aquaporin gene family of the ectomycorrhizal fungus *Laccaria bicolor*: lessons for symbiotic functions. *New Phytologist* 190: 927–940.
- Fan H, Dong H, Xu C, Liu J, Hu B, Ye J, Mai G, Li H. 2017. Pectin methyltransferases contribute the pathogenic differences between races 1 and 4 of *Fusarium oxysporum* f. sp. *cubense*. *Scientific Reports* 7: 13140.
- Federici L, Caprari C, Mattei B, Savino C, Di Matteo A, De Lorenzo G, Cervone F, Tsernoglou D. 2001. Structural requirements of endopolygalacturonase for the interaction with PGIIP (polygalacturonase-inhibiting protein). *Proceedings of the National Academy of Sciences, USA* 98: 13425–13430.
- Felten J, Kohler A, Morin E, Bhalerao RP, Palme K, Martin F, Ditetengou FA, Legué V. 2009. The ectomycorrhizal fungus *Laccaria bicolor* stimulates lateral root formation in poplar and Arabidopsis through auxin transport and signaling. *Plant Physiology* 151: 1991–2005.
- Ferrari S, Galletti R, Denoux C, De Lorenzo G, Ausubel FM, Dewdney J. 2007. Resistance to *Botrytis cinerea* induced in Arabidopsis by elicitors is independent of salicylic acid, ethylene, or jasmonate signaling but requires PHYTOALEXIN DEFICIENT3. *Plant Physiology* 144: 367–379.
- Ferrari S, Savatin DV, Sicilia F, Gramegna G, Cervone F, Lorenzo GD. 2013. Oligogalacturonides: plant damage-associated molecular patterns and regulators of growth and development. *Frontiers in Plant Science* 4: 49.
- García K, Delaux P-M, Cope KR, Ané J-M. 2015. Molecular signals required for the establishment and maintenance of ectomycorrhizal symbioses. *New Phytologist* 208: 79–87.
- Gea L, Normand L, Vian B, Gay G. 1994. Structural aspects of ectomycorrhiza of *Pinus pinaster* (Ait.) Sol. formed by an IAA-overproducer mutant of *Hebeloma cylindrosporum* Romagnési. *New Phytologist* 128: 659–670.
- Giovane A, Servillo L, Balestrieri C, Raiola A, D'Avino R, Tamburrini M, Ciardiello MA, Camardella L. 2004. Pectin methyltransferase inhibitor. *Biochimica et Biophysica Acta* 1696: 245–252.
- Glowacka K, Kromdijk J, Leonelli L, Niyogai KK, Clemente TE, Long SP. 2016. An evaluation of new and established methods to determine T-DNA copy number and homozygosity in transgenic plants. *Plant, Cell & Environment* 39: 908–917.
- Grsic-Rausch S, Rausch T. 2004. A coupled spectrophotometric enzyme assay for the determination of pectin methyltransferase activity and its inhibition by proteinaceous inhibitors. *Analytical Biochemistry* 333: 14–18.
- Hadfield KA, Bennett AB. 1998. Polygalacturonases: many genes in search of a function. *Plant Physiology* 117: 337–343.
- Hiremath S, McQuattie C, Podila G. 2013. Molecular marker genes for ectomycorrhizal symbiosis. *International Journal of Pharma and Bio Sciences* 4: 1075–1088.
- Hocq L, Pelloux J, Lefebvre V. 2017. Connecting homogalacturonan-type pectin remodeling to acid growth. *Trends in Plant Science* 22: 20–29.
- Juge N. 2006. Plant protein inhibitors of cell wall degrading enzymes. *Trends in Plant Science* 11: 359–367.
- Kemppainen M, Chowdhury J, Lundberg-Felten J, Pardo A. 2020. Fluorescent protein expression in the ectomycorrhizal fungus *Laccaria bicolor*: a plasmid toolkit for easy use of fluorescent markers in basidiomycetes. *Current Genetics* 66: 791–811.
- Kemppainen M, Circosta A, Tagu D, Martin F, Pardo AG. 2005. Agrobacterium-mediated transformation of the ectomycorrhizal symbiont *Laccaria bicolor* S238N. *Mycorrhiza* 16: 19–22.
- Kemppainen M, Duplessis S, Martin F, Pardo AG. 2008. T-DNA insertion, plasmid rescue and integration analysis in the model mycorrhizal fungus *Laccaria bicolor*. *Microbial Biotechnology* 1: 258–269.
- Kemppainen MJ, Pardo AG. 2010. Gene knockdown by ihpRNA-triggering in the ectomycorrhizal basidiomycete fungus *Laccaria bicolor*. *Bioengineered Bugs* 1: 354–358.
- Kim SJ, Zheng J, Hiremath ST, Podila GK. 1998. Cloning and characterization of a symbiosis-related gene from an ectomycorrhizal fungus *Laccaria bicolor*. *Gene* 222: 203–212.
- Kim Y, Teng Q, Wicker L. 2005. Action pattern of Valencia orange PME de-esterification of high methoxyl pectin and characterization of modified pectins. *Carbohydrate Research* 340: 2620–2629.
- Kohler A, Kuo A, Nagy LG, Morin E, Barry KW, Buscot F, Canbäck B, Choi C, Cichocki N, Clum A *et al.* 2015. Convergent losses of decay mechanisms and rapid turnover of symbiosis genes in mycorrhizal mutualists. *Nature Genetics* 47: 410–415.
- Kottke I, Oberwinkler F. 1987. The cellular structure of the Hartig net: coenocytic and transfer cell-like organization. *Nordic Journal of Botany* 7: 85–95.
- Lionetti V, Cervone F, Bellincampi D. 2012. Methyl esterification of pectin plays a role during plant-pathogen interactions and affects plant resistance to diseases. *Journal of Plant Physiology* 169: 1623–1630.
- Lionetti V, Raiola A, Camardella L, Giovane A, Obel N, Pauly M, Favaron F, Cervone F, Bellincampi D. 2007. Overexpression of pectin methyltransferase inhibitors in Arabidopsis restricts fungal infection by *Botrytis cinerea*. *Plant Physiology* 143: 1871–1880.
- Liu Y-G, Chen Y. 2007. High-efficiency thermal asymmetric interlaced PCR for amplification of unknown flanking sequences. *Biotechniques* 43: 649–650, 652, 654 passim.
- Liu YG, Mitsukawa N, Oosumi T, Whittier RF. 1995. Efficient isolation and mapping of *Arabidopsis thaliana* T-DNA insert junctions by thermal asymmetric interlaced PCR. *The Plant Journal* 8: 457–463.
- Ma L, Jiang S, Lin G, Cai J, Ye X, Chen H, Li M, Li H, Takács T, Samaj J *et al.* 2013. Wound-induced pectin methyltransferases enhance banana (*Musa* spp. AAA) susceptibility to *Fusarium oxysporum* f. sp. *cubense*. *Journal of Experimental Botany* 64: 2219–2229.
- Manmohit Kalia PK. 2015. Pectin methyltransferases: a review. *Journal of Bioprocessing & Biotechniques* 5. doi: 10.4172/2155-9821.1000227.
- Martin F, Aerts A, Ahrén D, Brun A, Danchin EGJ, Duchaussoy F, Gibon J, Kohler A, Lindquist E, Pereda V *et al.* 2008. The genome of *Laccaria bicolor* provides insights into mycorrhizal symbiosis. *Nature* 452: 88–92.
- Martin F, Kohler A, Murat C, Veneault-Fourrey C, Hibbett DS. 2016. Unearthing the roots of ectomycorrhizal symbioses. *Nature Reviews. Microbiology* 14: 760–773.
- Martin FM, Uroz S, Barker DG. 2017. Ancestral alliances: plant mutualistic symbioses with fungi and bacteria. *Science* 356. doi: 10.1126/science.aad4501.
- McGuire KL, Allison SD, Fierer N, Treseder KK. 2013. Ectomycorrhizal-dominated boreal and tropical forests have distinct fungal communities, but analogous spatial patterns across soil horizons. *PLoS ONE* 8: e68278.
- Micheli F. 2001. Pectin methyltransferases: cell wall enzymes with important roles in plant physiology. *Trends in Plant Science* 6: 414–419.
- Miyauchi S, Kiss E, Kuo A, Drula E, Kohler A, Sánchez-García M, Morin E, Andreopoulos B, Barry KW, Bonito G *et al.* 2020. Large-scale genome sequencing of mycorrhizal fungi provides insights into the early evolution of symbiotic traits. *Nature Communications* 11: 5125.
- Mouille G, Ralet M-C, Cavalier C, Eland C, Effroy D, Hématy K, McCartney L, Truong HN, Gaudon V, Thibault J-F *et al.* 2007. Homogalacturonan synthesis in *Arabidopsis thaliana* requires a golgi-localized protein with a putative methyltransferase domain. *The Plant Journal* 50: 605–614.
- Murashige T, Skoog F. 1962. A revised medium for rapid growth and bio assays with tobacco tissue cultures. *Physiologia Plantarum* 15: 473–497.
- Neb D, Das A, Hintelmann A, Nehls U. 2017. Composite poplars: a novel tool for ectomycorrhizal research. *Plant Cell Reports* 36: 1959–1970.
- Nguémazong DE, Jolie RP, Cardinaels R, Fraeye I, Van Loey A, Moldenaers P, Hendrickx M. 2012. Stiffness of Ca²⁺-pectin gels: combined effects of degree and pattern of methyltransferase for various Ca²⁺ concentrations. *Carbohydrate Research* 348: 69–76.

- Paris F, Dexheimer J, Lapeyrie F. 1993. Cytochemical evidence of a fungal cell wall alteration during infection of Eucalyptus roots by the ectomycorrhizal fungus *Cenococcum geophilum*. *Archives of Microbiology* 159: 526–529.
- Pelloux J, Rustérucci C, Mellerowicz EJ. 2007. New insights into pectin methylesterase structure and function. *Trends in Plant Science* 12: 267–277.
- Picelli S, Faridani OR, Björklund AK, Winberg G, Sagasser S, Sandberg R. 2014. Full-length RNA-seq from single cells using SMART-SEQ2. *Nature Protocols* 9: 171–181.
- Plett JM, Kempainen M, Kale SD, Kohler A, Legué V, Brun A, Tyler BM, Pardo AG, Martin F. 2011. A secreted effector protein of *Laccaria bicolor* is required for symbiosis development. *Current Biology* 21: 1197–1203.
- Plett JM, Tisserant E, Brun A, Morin E, Grigoriev IV, Kuo A, Martin F, Kohler A. 2015. The mutualist *Laccaria bicolor* expresses a core gene regulon during the colonization of diverse host plants and a variable regulon to counteract host-specific defenses. *Molecular Plant–Microbe Interactions* 28: 261–273.
- Podila GK, Zheng J, Balasubramanian S, Sundaram S, Hiremath S, Brand JH, Hymes MJ. 2002. Fungal gene expression in early symbiotic interactions between *Laccaria bicolor* and red pine. In: Smith SE, Smith FA, eds. *Diversity and integration in mycorrhizas*. Dordrecht, the Netherlands: Springer, 117–128.
- Protsenko MA, Buza NL, Krinitsyna AA, Bulantseva EA, Korableva NP. 2008. Polygalacturonase-inhibiting protein is a structural component of plant cell wall. *Biochemistry. Biokhimiia* 73: 1053–1062.
- Qu L, Makoto K, Choi DS, Quoreishi AM, Koike T. 2010. The role of ectomycorrhiza in boreal forest ecosystem. In: Osawa A, Zyryanova OA, Matsuura Y, Kajimoto T, Wein RW, eds. *Ecological studies. Permafrost ecosystems*. Dordrecht, the Netherlands: Springer, 413–425.
- Ralet M-C, Dronnet V, Buchholt HC, Thibault J-F. 2001. Enzymatically and chemically de-esterified lime pectins: characterisation, polyelectrolyte behaviour and calcium binding properties. *Carbohydrate Research* 336: 117–125.
- Read DJ, Leake JR, Perez-Moreno J. 2004. Mycorrhizal fungi as drivers of ecosystem processes in heathland and boreal forest biomes. *Canadian Journal of Botany* 82: 1243–1263.
- Reca IB, Lionetti V, Camardella L, D'Avino R, Giardina T, Cervone F, Bellincampi D. 2012. A functional pectin methylesterase inhibitor protein (SolyPMEI) is expressed during tomato fruit ripening and interacts with PME-1. *Plant Molecular Biology* 79: 429–442.
- Sebastiana M, Vieira B, Lino-Neto T, Monteiro F, Figueiredo A, Sousa L, Pais MS, Tavares R, Paulo OS. 2014. Oak root response to ectomycorrhizal symbiosis establishment: RNA-Seq derived transcript identification and expression profiling. *PLoS ONE* 9: e98376.
- Sella L, Castiglioni C, Paccanaro MC, Janni M, Schäfer W, D'Ovidio R, Favaron F. 2016. Involvement of fungal pectin methylesterase activity in the interaction between *Fusarium graminearum* and wheat. *Molecular Plant–Microbe Interactions* 29: 258–267.
- Sénéchal F, L'Enfant M, Domon JM, Rosiau E, Crépeau MJ, Surcouf O, Esquivel-Rodriguez J, Marcelo P, Mareck A, Guérineau F *et al.* 2015. Tuning of pectin methylesterification: PECTIN METHYLESTERASE INHIBITOR 7 modulates the processive activity of co-expressed PECTIN METHYLESTERASE 3 in a pH-dependent manner. *The Journal of Biological Chemistry* 290: 23320–23335.
- Sénéchal F, Wattier C, Rustérucci C, Pelloux J. 2014. Homogalacturonan-modifying enzymes: structure, expression, and roles in plants. *Journal of Experimental Botany* 65: 5125–5160.
- Sillo F, Fangel JU, Henrissat B, Faccio A, Bonfante P, Martin F, Willats WGT, Balestrini R. 2016. Understanding plant cell-wall remodelling during the symbiotic interaction between *Tuber melanosporum* and *Corylus avellana* using a carbohydrate microarray. *Planta* 244: 347–359.
- Sundell D, Mannapperuma C, Netotea S, Delhomme N, Lin Y-C, Sjödin A, Van de Peer Y, Jansson S, Hvidsten TR, Street NR. 2015. The plant genome integrative explorer resource: plantgenie.org. *New Phytologist* 208: 1149–1156.
- Veneault-Fourrey C, Commun C, Kohler A, Morin E, Balestrini R, Plett J, Danchin E, Coutinho P, Wiebenga A, de Vries RP *et al.* 2014. Genomic and transcriptomic analysis of *Laccaria bicolor* CAZome reveals insights into polysaccharides remodelling during symbiosis establishment. *Fungal Genetics and Biology* 72: 168–181.
- Veneault-Fourrey C, Martin F. 2011. Mutualistic interactions on a knife-edge between saprotrophy and pathogenesis. *Current Opinion in Plant Biology* 14: 444–450.
- Verherbruggen Y, Marcus SE, Haeger A, Ordaz-Ortiz JJ, Knox JP. 2009. An extended set of monoclonal antibodies to pectic homogalacturonan. *Carbohydrate Research* 344: 1858–1862.
- Verlent I, Smout C, Duvetter T, Hendrickx ME, Van Loey A. 2005. Effect of temperature and pressure on the activity of purified tomato polygalacturonase in the presence of pectins with different patterns of methyl esterification. *Innovative Food Science & Emerging Technologies* 6: 293–303.
- Wilson SM, Bacic A. 2012. Preparation of plant cells for transmission electron microscopy to optimize immunogold labeling of carbohydrate and protein epitopes. *Nature Protocols* 7: 1716–1727.
- Wolf S, Mouille G, Pelloux J. 2009. Homogalacturonan methyl-esterification and plant development. *Molecular Plant* 2: 851–860.
- Wormit A, Usadel B. 2018. The multifaceted role of pectin methylesterase inhibitors (PMEIs). *International Journal of Molecular Sciences* 19: 2878.
- Zhang F, Anasztzisz GE, Labourel A, Champion C, Haon M, Kempainen M, Commun C, Deveau A, Pardo A, Veneault-Fourrey C *et al.* 2018. The ectomycorrhizal basidiomycete *Laccaria bicolor* releases a secreted β -1,4 endoglucanase that plays a key role in symbiosis development. *New Phytologist* 220: 1309–1321.
- Zhang F, Labourel A, Haon M, Kempainen M, Da Silva ME, Brouilly N, Veneault-Fourrey C, Kohler A, Rosso M-N, Pardo A *et al.* 2022. The ectomycorrhizal basidiomycete *Laccaria bicolor* releases a GH28 polygalacturonase that plays a key role in symbiosis establishment. *New Phytologist* 233: 2534–2547.

Supporting Information

Additional Supporting Information may be found online in the Supporting Information section at the end of the article.

Fig. S1 Schematic diagram of vector constructs used in this study for altering *Laccaria bicolor* PME expression.

Fig. S2 qPCR screening of *Laccaria bicolor* RNAi and overexpressor (OE) transformant lines for PME expression in free-living mycelium.

Fig. S3 Gradual development of *Laccaria bicolor* colonisation whilst interacting with *Populus tremula* × *Populus tremuloides* lateral roots at various days after contact (DAC) under the *in vitro* sandwich culture system.

Fig. S4 Venn diagrams of differentially expressed genes (DEGs) (P -adj < 0.01; \log_2 fold change > 0.5) in mycelium in ECM compared with free-living mycelium.

Fig. S5 Proportion of differentially expressed and unchanged cell-wall-degrading enzymes (CWDEs) among key gene families in *Populus tremula* × *Populus tremuloides* and *Laccaria bicolor* potentially play crucial roles during ECM formation.

Fig. S6 Proportion of differentially expressed genes and unchanged genes associated with specific polysaccharide degrading enzymes in *Populus tremula* × *Populus tremuloides* and *Laccaria bicolor*.

Fig. S7 Time-course RNA-seq expression profile of the potential candidates of HG synthesis and modifying enzymes (HGMEs) during *Laccaria bicolor*/ *Populus tremula* × *Populus tremuloides* interaction.

Fig. S8 Comparison of gene-expression values obtained by RT-qPCR and RNA-seq.

Fig. S9 Time-course RNA-seq expression profile of four *Laccaria bicolor* PMEs in colonised roots (ECM) and free-living mycelia (FLM).

Fig. S10 Phylogenetic relationship of PME and PME inhibitor (PMEI) proteins from *Populus tremula* (reference genome for *P. tremula* × *P. tremuloides*) and fungi.

Fig. S11 Differential expression of *Populus tremula* × *Populus tremuloides* HG biosynthesis genes during interaction with *Laccaria bicolor* based on RNA-seq data from our study.

Fig. S12 Comparison of differentially expressed Lb CAZymes in our study to those in Veneault-Fourrey *et al.* (2014); Plett *et al.* (2015) during interaction of *Populus* with *Laccaria bicolor* in a soil system.

Fig. S13 Immunolocalisation with pectin antibodies LM19 and LM20 at various distances from the root tips.

Fig. S14 Transmission electron micrographs of immunogold labelling of homogalacturonan epitopes present in the epidermis cell wall of ECM and control root cross-sections.

Fig. S15 Quantification of gold particles in the Hartig net plant cell wall and corresponding cell-wall areas of control roots on TEM image.

Fig. S16 PME activity of pooled lateral roots collected from *Populus tremula* × *Populus tremuloides*/*Laccaria bicolor* colonised roots at 14 d after contact, control roots without fungus and free-living mycelia.

Fig. S17 Multiple sequence alignment and sequence identity of *Laccaria bicolor* PME proteins.

Fig. S18 Relative normalised expression of *LbPG* in free-living mycelia of the PME transgenic lines by qPCR.

Fig. S19 Correlation of *PME1* transcript level and PME enzymatic activity level in the free-living mycelia of the transgenic fungal lines.

Fig. S20 Examples of control roots and swollen root tips with attachment of fungal mycelia on colonised roots.

Fig. S21 Representative micrographs of sections through ectomycorrhizal root tips of *Populus tremula* × *Populus tremuloides* in contact with *Laccaria bicolor* wild-type, empty vector line 7, *PME1* RNAi line 21, *PME* double RNAi line 10 and *PME1* overexpressor line 47.

Fig. S22 Model of pectin modification during Hartig net formation in *Laccaria bicolor*/*Populus* interaction.

Methods S1 Bioinformatics.

Methods S2 PME activity assay in free-living mycelium.

Methods S3 Immunofluorescence localisation of pectin antibodies in poplar roots.

Methods S4 Cloning, *Laccaria bicolor* transformation and fungal selection.

Methods S5 Characterisation of T-DNA insertion number in transgenic *Laccaria bicolor* lines by ddPCR.

Methods S6 Characterisation of T-DNA insertion sites in transgenic *Laccaria bicolor* by plasmid rescue and TAIL PCR.

Methods S7 Characterisation of T-DNA insertion number in transgenic *Laccaria bicolor* lines by ddPCR.

Table S1 List of primer sequences used in this study.

Table S2 Genomic T-DNA insertion number and integration sites in *Laccaria bicolor* transformants used in this study.

Table S3 Gene-expression data of *Laccaria bicolor* (based on JGI genome v.2.0 annotation) ectomycorrhiza vs free-living mycelium.

Table S4 Gene-expression data from *P. tremula* × *P. tremuloides* annotated based on the *P. tremula* genome, ectomycorrhiza vs control root.

Table S5 *Laccaria bicolor* genes specifically differentially expressed at only one of the time points during the interaction (P -adj < 0.01; log₂ fold change > 0.5).

Table S6 *Populus* genes specifically differentially expressed at only one of the time points during the interaction (P -adj < 0.01; log₂ fold change > 0.5).

Table S7 Differentially expressed (P -adj < 0.01; log₂ fold change > 0.5) *Laccaria bicolor* CAZymes in our study compared with literature studies by Veneault-Fourrey *et al.* (2014); Plett *et al.* (2015).

Table S8 Differentially expressed (P -adj < 0.01; log₂ fold change > 0.5) *Populus tremula* × *Populus tremuloides* CAZymes in our study.

Please note: Wiley Blackwell are not responsible for the content or functionality of any Supporting Information supplied by the authors. Any queries (other than missing material) should be directed to the *New Phytologist* Central Office.